

AD-A019 503

INVESTIGATION OF $K(o)$ TESTING IN COHESIONLESS SOILS

Mosaïd M. Al-Hussaini, et al

Army Engineer Waterways Experiment Station
Vicksburg, Mississippi

December 1975

DISTRIBUTED BY:

NTIS

National Technical Information Service
U. S. DEPARTMENT OF COMMERCE

023088



TECHNICAL REPORT S-75-16

INVESTIGATION OF K_0 TESTING IN COHESIONLESS SOILS

by

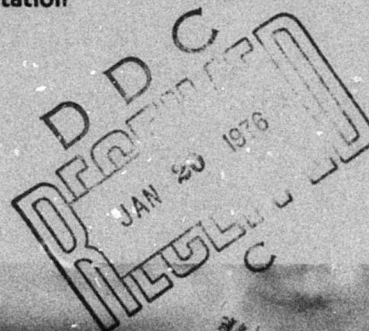
Mosaid M. Al-Hussaini, Frank C. Townsend

Soils and Pavements Laboratory
U. S. Army Engineer Waterways Experiment Station
P. O. Box 631, Vicksburg, Miss. 39180

December 1975

Final Report

Approved For Public Release; Distribution Unlimited



Prepared for Assistant Secretary of the Army (R&D)
Washington, D. C. 20314

Under Project No. 4A061101A9ID

Reproduced by
**NATIONAL TECHNICAL
INFORMATION SERVICE**
US Department of Commerce
Springfield, VA. 22151

Unclassified

SECURITY CLASSIFICATION OF THIS PAGE (When Data Entered)

REPORT DOCUMENTATION PAGE		READ INSTRUCTIONS BEFORE COMPLETING FORM
1. REPORT NUMBER Technical Report S-75-16	2. GOVT ACCESSION NO.	3. RECIPIENT'S CATALOG NUMBER
4. TITLE (and Subtitle) INVESTIGATION OF K_0 TESTING IN COHESIONLESS SOILS		5. TYPE OF REPORT & PERIOD COVERED Final report
		6. PERFORMING ORG. REPORT NUMBER
7. AUTHOR(s) Mosaid M. Al-Hussaini Frank C. Townsend		8. CONTRACT OR GRANT NUMBER(s)
9. PERFORMING ORGANIZATION NAME AND ADDRESS U. S. Army Engineer Waterways Experiment Station Soils and Pavements Laboratory P. O. Box 631, Vicksburg, Miss. 39180		10. PROGRAM ELEMENT, PROJECT, TASK AREA & WORK UNIT NUMBERS Project No. 4A061101A91D
11. CONTROLLING OFFICE NAME AND ADDRESS Assistant Secretary of the Army (R&D) Washington, D. C. 20314		12. REPORT DATE December 1975
		13. NUMBER OF PAGES 72
14. MONITORING AGENCY NAME & ADDRESS (if different from Controlling Office)		15. SECURITY CLASS. (of this report) Unclassified
		15a. DECLASSIFICATION/DOWNGRADING SCHEDULE
16. DISTRIBUTION STATEMENT (of this Report) Approved for public release; distribution unlimited.		
17. DISTRIBUTION STATEMENT (of the abstract entered in Block 20, if different from Report)		
18. SUPPLEMENTARY NOTES		
19. KEY WORDS (Continue on reverse side if necessary and identify by block number) Coefficient of earth pressure Soil tests Earth pressure Stress-strain relations (soils) Noncohesive soils Sands		
20. ABSTRACT (Continue on reverse side if necessary and identify by block number) The ratio of horizontal to vertical effective stress when lateral yielding is prevented is known as the coefficient of earth pressure at rest and is denoted by the symbol K_0 . K_0 values and the stress-strain response of soils under conditions of lateral restraint are important engineering quantities for problems involving settlement of large fills, lateral pressures on retaining structures, and yielding around excavations. In this report, four laboratory techniques and devices for experimentally determining K_0 values and (Continued)		

DD FORM 1 JAN 73 1473 EDITION OF 1 NOV 65 IS OBSOLETE

Unclassified

SECURITY CLASSIFICATION OF THIS PAGE (When Data Entered)

Unclassified

SECURITY CLASSIFICATION OF THIS PAGE(When Data Entered)

20. ABSTRACT (Continued).

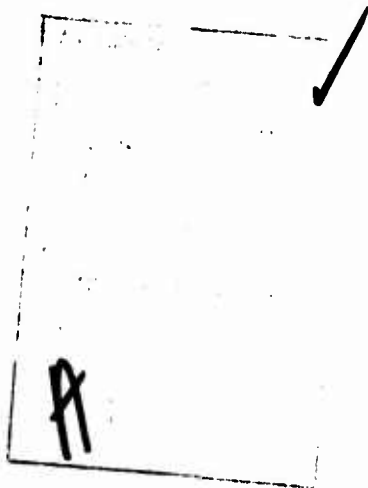
the stress-strain relationships of Reid-Bedford sand are examined. These methods are: the linear variable displacement transducer (LVDT) clamp, the K_0 belt, swinging arms lateral strain sensors, and an indirect volume change method using a burette. The tests were conducted at three relative densities, 25, 75, and 100 percent, using modified triaxial compression chambers. The test results showed that the value of K_0 for Reid-Bedford sand was practically the same irrespective of the testing method and equipment and that it decreased with increasing relative density. The experimentally measured K_0 values agreed well with Jaky's theoretical equation, $K_0 = 1 - \sin \phi$, where ϕ is the angle of internal friction. K_0 values determined by dynamic techniques in another study agreed favorably with values derived in this study, thus suggesting that K_0 and the stress-strain relationships under K_0 conditions are insensitive to rate of loading. The constrained modulus, D , increased with increasing density and stress level. The swinging arms lateral strain sensor gave the highest constrained modulus values, while the LVDT clamp gave the lowest. The effect of stress history on the value of K_0 was also examined in this study. Loading and unloading tests under K_0 conditions using the LVDT clamps revealed that K_0 values were lower on loading than unloading and increased with increasing number of loading cycles. These results suggest that K_0 is stress history-dependent. These tests further showed that K_0 values increased with increasing stress level and that this increase was more pronounced in dense rather than loose sand. The constrained modulus D increased with increasing number of loading cycles, yet D was much higher on unloading and was practically the same for each unloading cycle.

Unclassified

SECURITY CLASSIFICATION OF THIS PAGE(When Data Entered)

Destroy this report when no longer needed. Do not return
it to the originator.

THE CONTENTS OF THIS REPORT ARE NOT TO BE
USED FOR ADVERTISING, PUBLICATION, OR
PROMOTIONAL PURPOSES. CITATION OF TRADE
NAMES DOES NOT CONSTITUTE AN OFFICIAL EN-
FORCEMENT OR APPROVAL OF THE USE OF SUCH
COMMERCIAL PRODUCTS.



PREFACE

The investigation reported herein was conducted under Department of the Army Project No. 4A061101A91D, In-House Laboratory Independent Research (ILIR) Program, sponsored by the Assistant Secretary of the Army (R&D). Authorization for the study was initially granted by WESVB Disposition Form, dated 2 February 1972, subject: "In-House Laboratory Independent Research Program FY 1973." Authorization for continuation during 1974 was granted by WESVB Disposition Form, dated 2 June 1973, subject: "In-House Laboratory Independent Research Program FY 1974." This investigation was conducted during the period August 1973-June 1974 in the Soils and Pavements Laboratory, U. S. Army Engineer Waterways Experiment Station (WES).

A one-dimensional compression testing device was designed at WES, and the investigation was conducted by Dr. Mosaid M. Al-Hussaini assisted by Mr. Willie J. Hughes, both of the Soils Research Facility. This report was prepared by Dr. Al-Hussaini and Dr. Frank C. Townsend, Chief, Soils Research Facility, under the general supervision of Mr. Clifford L. McAnear, Chief, Soil Mechanics Division, and Mr. J. P. Sale, Chief, Soils and Pavements Laboratory.

Director of WES during the investigation and preparation of this report was COL G. H. Hilt, CE. Technical Director was Mr. F. R. Brown.

CONTENTS

	<u>Page</u>
PREFACE	2
CONVERSION FACTORS, U. S. CUSTOMARY TO METRIC (SI)	
UNITS OF MEASUREMENT	4
PART I: INTRODUCTION	5
Background	5
Objectives and Scope of Study	6
PART II: LITERATURE REVIEW	7
Scale Model Testing	7
Laboratory Testing	9
Field Measurement of K_o	20
Theoretical Evaluation of K_o	27
PART III: MATERIAL, TESTING EQUIPMENT, AND PROCEDURES	32
Material	32
Testing Equipment	33
Test Procedures	41
PART IV: TEST RESULTS AND DISCUSSION OF EXPERIMENTAL RESULTS . .	43
Coefficient of Earth Pressure at Rest K_o	43
Stress-Strain Relationship	50
Factors Affecting K_o and Constrained Modulus	52
PART V: CONCLUSIONS AND RECOMMENDATIONS	66
Conclusions	66
Recommendations	67
REFERENCES	68
APPENDIX A: NOTATION	

CONVERSION FACTORS, U. S. CUSTOMARY TO METRIC (SI)
UNITS OF MEASUREMENT

U. S. customary units of measurement used in this report can be converted to metric (SI) units as follows:

<u>Multiply</u>	<u>By</u>	<u>To Obtain</u>
inches	2.54	centimetres
feet	0.3048	metres
miles (U. S. statute)	1.609344	kilometres
pounds (force) per square inch	6894.757	pascals
kips per square inch	6.894757×10^6	pascals

INVESTIGATION OF K_0 TESTING IN COHESIONLESS SOILS

PART I: INTRODUCTION

Background

1. The ratio of horizontal to vertical stress when lateral yielding is prevented is known as the coefficient of earth pressure at rest and is denoted by the symbol K_0 .^{*} For elastic isotropic materials under first loading, the value of K_0 can be expressed directly in terms of Poisson's ratio ν , e.g., $K_0 = \nu / (1 - \nu)$. Consequently, K_0 can be considered as an elastic soil parameter. Many naturally occurring sediments as well as man-made fills are deposited and compacted in almost horizontal layers where little or no lateral yielding occurs. Hence the value of K_0 and stress-strain response of soils under conditions of lateral restraint are important engineering considerations for problems involving settlement of large fills, lateral pressures on nonyielding retaining structures, and excavations. Furthermore, since K_0 is an elastic soil parameter, a knowledge of K_0 is applicable to static problems and many dynamic problems, e.g., the displacement in laterally confined strata due to one-dimensional wave propagation.

2. The measurement of K_0 in the laboratory as well as in the field has always been of interest to engineers since stresses under K_0 conditions play a major role in the behavior of soil. Many methods and testing devices have been developed for determining uniaxial stress-strain and K_0 values. In this context, the problem is to determine which method and technique provide the best estimate of K_0 and what factors significantly affect the measured values.

* For convenience, symbols and unusual abbreviations are listed and defined in the Notation (Appendix A).

Objectives and Scope of Study

3. The purpose of this study was to examine various experimental and analytical methods used in evaluating K_0 , Poisson's ratio, and the stress-strain behavior of sands in one-dimensional compression. The various factors which affect granular soil behavior under one-dimensional compression were also investigated.

4. Because it is practically impossible to study the performance of every device developed for measuring K_0 in the laboratory, only four devices were selected for this comparative study. The selected methods and equipment were (a) the linear variable displacement transducer (LVDT) clamp, (b) the lateral strain sensor with strain gages, (c) the indirect method which uses a burette to measure volume change, and (d) swinging arms with external LVDT. Several granular materials were selected for the test program; however, the bulk of the data was generated from testing sand known locally as Reid-Bedford sand. Specimens of Reid-Bedford sand were prepared at three densities--loose, medium dense, and dense--and loaded in a triaxial compression device under K_0 conditions.

PART II: LITERATURE REVIEW

5. The purpose of this part is to review some of the significant experimental and theoretical work on one-dimensional compression (i.e., K_0) characteristics of soils. All the work which has contributed to the understanding of the behavior of soil under K_0 conditions is not included; only those investigations which seemed pertinent to this study are reviewed.

Scale Model Testing

Experiments with retaining walls

6. The idea of testing soil under K_0 conditions is not new. In fact, early tests on soil under no lateral yield were performed on full-scale retaining walls in an effort to examine the effect of outward yielding on the horizontal thrust exerted on the wall by the retained soil. In early 1934, Terzaghi¹ presented test data on a model retaining wall 7 ft* high and 14 ft wide which could be moved inward, outward, or tilted around the lower edge. Results on compacted sand showed that inward movement of the wall for a distance of $0.001 h$ (where h is the depth of the fill) increased the ratio of lateral soil pressure to the assumed hydrostatic pressure by 2-2.5 times, while outward movement by the same amount decreased the lateral pressure ratio to about 0.1 over that of a nonyielding wall. Rinkert² conducted studies on a reinforced concrete cantilever retaining wall 2.0 m high, 6.0 m long, and 0.2 m wide. The wall surface was covered with sheet metal coated with grease to reduce wall friction with the filling material. Two materials were used in the test program. One material was crushed stone ranging from 3.2 to 6.4 cm in diameter, and the other was rounded pebbles ranging from 1.6 to 3.2 cm in diameter. The results showed that an average outward movement of $1/3000$ of the wall height for the crushed

* A table of factors for converting U. S. customary units of measurement to metric (SI) units is presented on page 4.

stone and 1/800 of the wall height for the pebbles was sufficient to induce an active state of stress in the backfill material.

Effect of lateral movement

7. The studies by Terzaghi and Rinkert demonstrated the dependency of the lateral earth pressure of a backfill material on the amount and direction of yielding of a retaining structure. They clearly indicated that very small movements in the retaining wall may change the state of stress in the fill material to either the passive or active state of stress, depending on the direction of movement. The variation of the coefficient of earth pressure with respect to wall movement is shown in Figure 1. Of course the shape of the curve is not unique, but is strongly influenced by the type of soil and its physical characteristics at the time of the test. The important conclusion which can be derived from this figure is that very little expansive horizontal strain is required to reach the active Rankine state, while much more compressive horizontal strain is required to reach passive Rankine state. The ratio

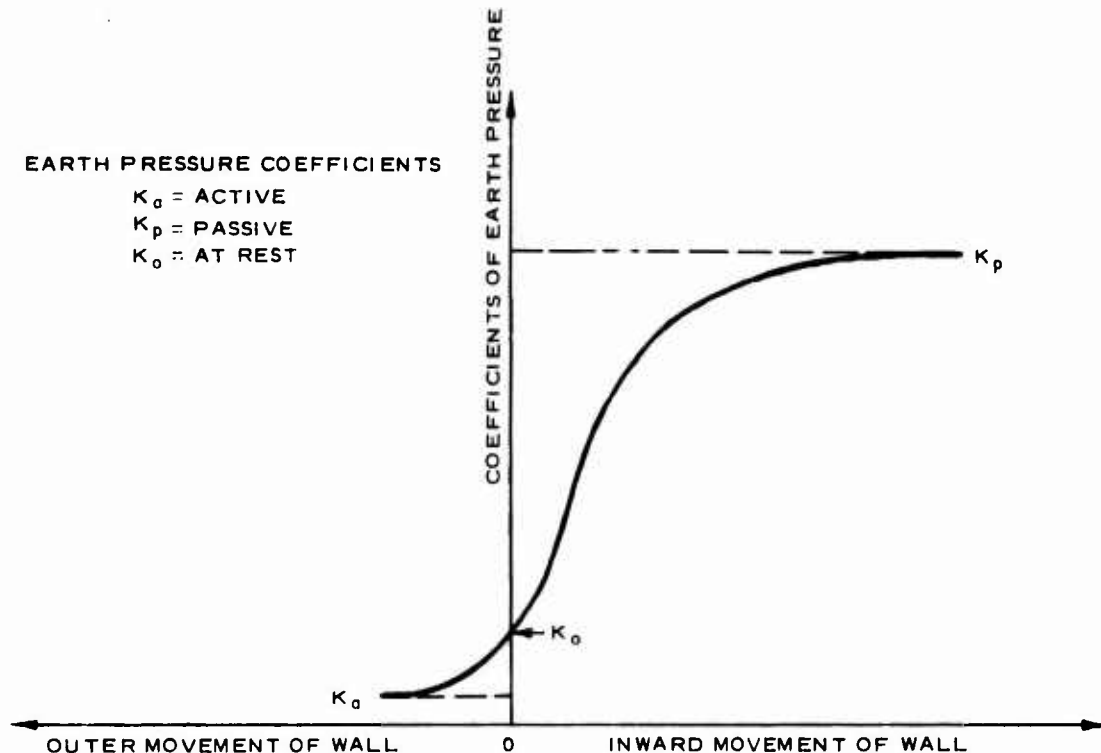


Figure 1. Earth pressure coefficient versus lateral yield

of the horizontal strains for the passive state to those of the active state varies with density of material and type of soil considered. According to Mackey and Kirk,³ this ratio may vary from about 4 for dense sand increasing to about 30 for loose sand.

8. The classic method of designing retaining walls, which is still practiced by many designers, is to assume that the soil behind the retaining wall is in an active state of stress regardless of the magnitude of the movement required to produce the active state of stress. In cases in which the magnitude of lateral movement is limited, the assumption of an active state of stress could be dangerous since this assumption greatly underestimates the magnitude of the actual lateral pressure acting on the wall. The knowledge of the value of K_0 in such cases is vital.

Laboratory Testing

9. Two conditions must be satisfied in testing soils under K_0 conditions: (a) lateral yielding must be of negligible magnitude and (b) the soil must deform freely in the axial direction (i.e., no friction or other interference from the testing equipment). Previous investigators have employed numerous devices and methods for testing soils; some of the devices are described herein.

Classic methods

10. Probably the first apparatus used in determining earth pressure at rest for sand was the one described by Terzaghi.⁴ The apparatus consisted of a rigid square frame with one side separated from the other sides by a small gap to allow the passage of a steel tape as shown in Figure 2. The sand was placed in the rigid frame, covered with a rigid plate, and subjected to vertical pressures in a testing machine. The lateral pressure was transmitted to the steel tape through a sheet of paper. The coefficient of friction between the steel tape and the paper was established by calibration procedures; hence, the lateral pressure in the sand could be calculated from the force necessary to overcome the friction of the tape. Terzaghi stated that "even this primitive

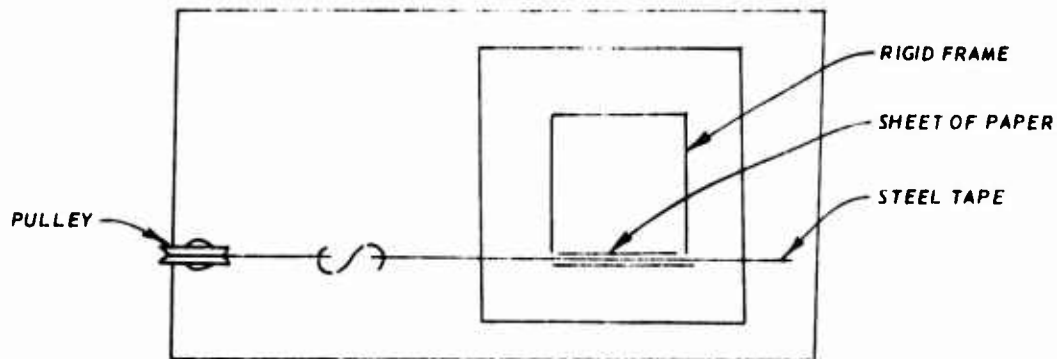


Figure 2. Terzaghi apparatus for determining earth pressure at rest

apparatus furnished very satisfactory results."

11. The coefficient of earth pressure at rest was measured in 1936 by Kjellman⁵ in an apparatus which enabled the three principal stresses to be varied on a 6.2-cm cubical specimen as shown in Figure 3. One hundred rods on each side were used, each rod being 0.6 by 0.6 by 3.2 cm, with one end resting on a rubber membrane surrounding the specimen while the other end was forced against a steel plate. The amount of

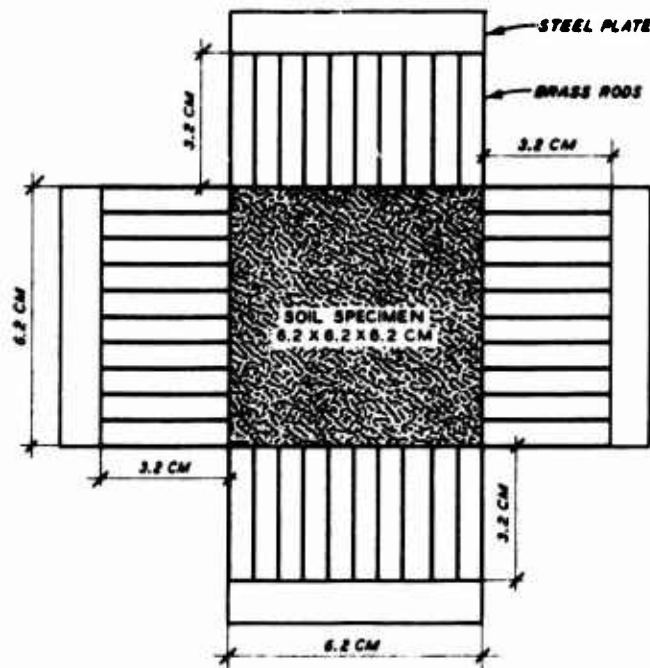


Figure 3. Triaxial apparatus by Kjellman (courtesy of Harvard University Press⁵)

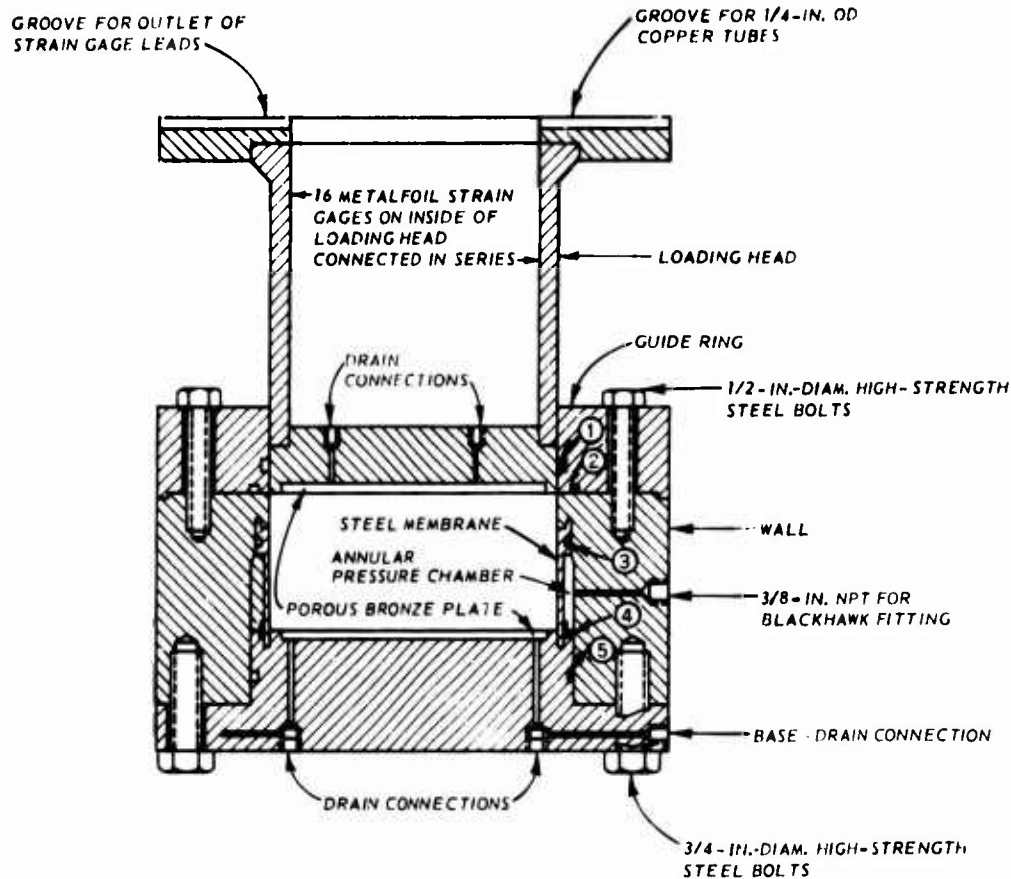
stress applied on each side of the specimen was calculated from the measurements of the total force applied to the rods, and the deformation within the soil was calculated from the relative movement of each steel plate from its original position. The apparatus was not widely used simply because of the difficulties involved in preparing the specimen. The significant observation from the Kjellman test was that the value of K_0 was found to increase with increasing overconsolidation ratio for sand.

Modern techniques

12. Since the early experimental work of Terzaghi and Kjellman for determining the coefficient of earth pressure at rest, many new techniques and devices for measuring K_0 have evolved. These new procedures can be divided into the following categories:

- a. Modified odometer test
- b. Modified triaxial compression test
- c. Indirect or burette method
- d. Other methods

13. Modified odometer method. A high-pressure one-dimensional consolidometer in which the axial and lateral pressures could be measured was designed at the University of Illinois by Hendron⁶ for testing sand. To accommodate saturated clay, the apparatus was slightly modified by Brooker and Ireland⁷ who added pore pressure measuring components to the original device. The modified K_0 device, shown in Figure 4, consisted essentially of a flexible, thin steel ring which contained the soil specimen (6.8 in. in diameter and 2 in. high) surrounded by an annular space that could be filled with oil from a hydraulic system. The flexible ring and the oil space were surrounded by a thick, hollow cylinder bolted to a base and guide ring. As the axial load was applied to the soil specimen, the strain in the surrounding steel ring was registered by four strain gages mounted on the ring. In order to maintain null strain conditions in the ring, the oil pressure was continuously modified by two solenoid valves to compensate for the change due to the vertical load. With the exception of friction caused by the confining ring, the apparatus may be considered as the most



NOTE ① TO ⑤ ARE O-RING SEALS.

Figure 4. University of Illinois K_0 apparatus (after Reference 7) suitable for testing soil under high pressure.

14. Modified triaxial compression test. In view of difficulties associated with side friction and in placing undisturbed samples containing small stones in the conventional consolidometer, a special K_0 testing apparatus was devised by Murdock.⁸ The apparatus used was a modified triaxial compression apparatus in which a sensing device was added to detect the change in the diameter of the soil specimen during testing. The sensing device consisted of a thin metal band with an adjustable contact screw and two wires leading to a battery and lamp as shown in Figure 5. As axial load was applied to the specimen, any tendency on the part of the specimen to bulge caused breaking of the electrical contact and put out the light. This small change in diameter was

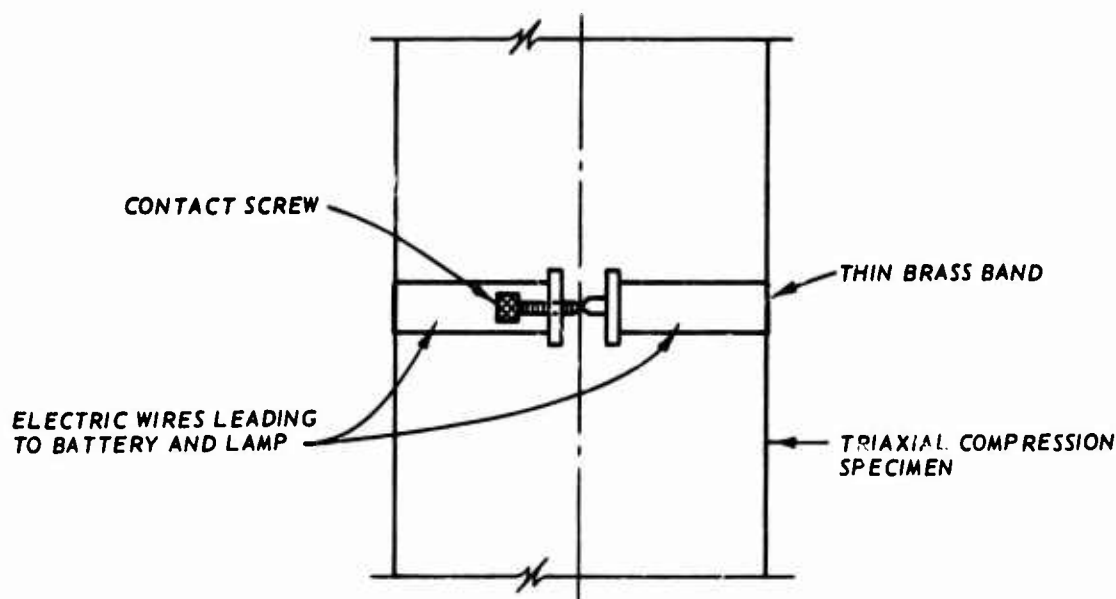


Figure 5. Murdock sensing device as adapted to triaxial compression test

negated by increasing the cell pressure until the light came on again. The process then continued to the end of the test.

15. In 1958 Bishop⁹ described an indicator for testing 4-in.-diam specimens under K_0 conditions using the conventional triaxial test. The lateral indicator, as shown in Figure 6, consisted of two curved aluminum strips joined by a low friction hinge on one end and a mercury pot with diaphragm on the other end. The lateral indicator was also provided with metal pads which bore gently on the midheight periphery of the sample and were held in position by contact friction. The radial deformation of the specimen could be sensed by the movement of mercury column in a calibrated transparent tube. K_0 test procedure consisted of increasing the axial and radial stresses slowly so that no movement in the column of mercury was allowed, thus insuring no change in the diameter of the specimen.

16. Because of the difficulties as well as the danger of toxicity involved in dealing with mercury, many modifications of Bishop's lateral indicator have been developed. A lateral deformation sensor similar to that developed by Bishop was developed at the University of

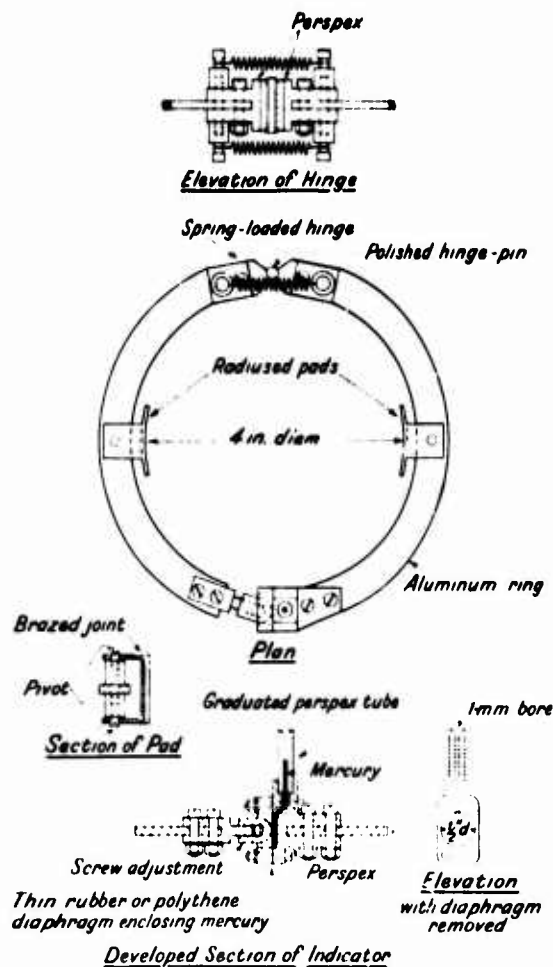


Figure 6. Bishop's lateral strain indicator (from Reference 9)

California at Berkeley^{10,11} in connection with their studies on cyclic triaxial compression tests. The main difference between the two devices is that the mercury pot used by Bishop was replaced by an LVDT in the device used at Berkeley. This type of lateral deformation sensor provided a satisfactory K_0 value for dense sand and firm clay; however, in testing loose sand and soft clay the device may be deficient in two respects. First, slippage of the clamp during testing may indicate lateral deformation in the specimen when in reality there is no lateral deformation; this is a minor problem and can be corrected easily by gluing the points of contact of the device to the rubber membrane. The

second problem is that loose sand and soft clay may yield at points of contact between the specimen and the sensor. This problem can be solved by enlarging the contact surface area or by using another lateral deformation sensing device called the K_0 belt. A lateral deformation sensing device similar to that used at Berkeley was constructed at the U. S. Army Engineer Waterways Experiment Station (WES) and has been selected for comparative study and evaluation in this report.

17. The K_0 belt has been used at WES to obtain K_0 values for granular materials. The K_0 belt consisted of a thin metal band instrumented with four strain gages and placed around the middle of triaxial specimens; more detailed description of the device is presented in Reference 12. The WES K_0 belt was used in this study, and the results will be presented in later parts of this report. Another K_0 belt which is similar in many respects to the WES K_0 belt was described by Moore.¹³

18. Indirect method or burette method. A simple procedure for simulating K_0 consolidation in the conventional triaxial apparatus has been developed by Bishop and Eldin.¹⁴ The test procedure, as illustrated in Figure 7, is based on the assumption that the volume of water

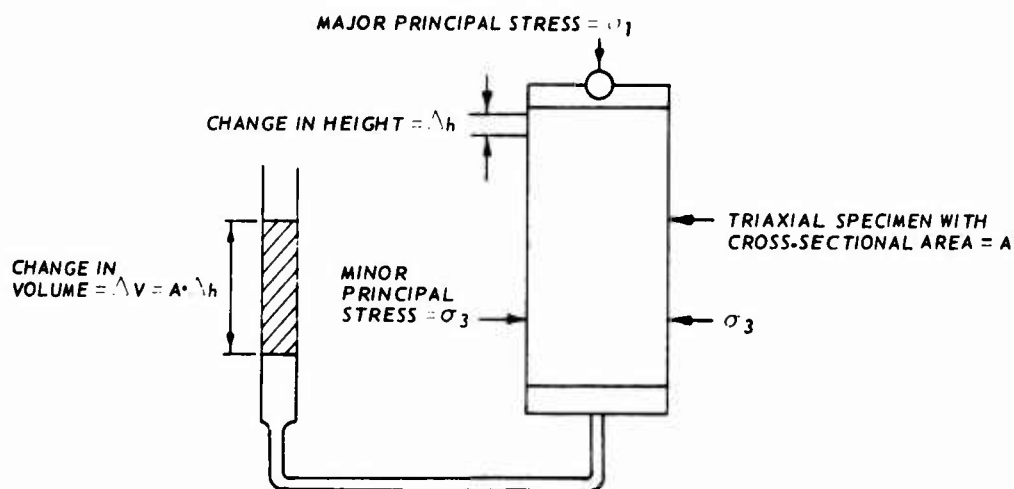


Figure 7. Illustration of volume change concept in K_0 testing

expelled from a saturated specimen with no radial deformation is equal to the initial area of the specimen multiplied by the change in its

height. Therefore, K_0 conditions could be maintained by increasing the radial and axial stresses such that the volume change indicated by the burette corresponds to the vertical deformation of the sample. The most attractive feature of the indirect test method is its simplicity. The device requires nothing more than a burette, which is usually incorporated in most triaxial cells, for measuring volume change. For this reason alone, the test was chosen for comparison with other testing techniques presented in this study. The test, however, has been criticized by Andrawes and El-Sohby¹⁵ as it takes a long time to conduct the test on cohesive soil in which no appreciable hydraulic gradient is allowed. The test procedure is not applicable for testing partially saturated clay or dry sand. In tests of saturated granular soil, careful correction should be made to the volume change due to both membrane penetration and water evaporation from the burette.

19. Modified triaxial apparatus with swinging arms. A new device for consolidating cylindrical specimens of cohesive soil under K_0 conditions was developed at Purdue University. The device, as described by Holtz,¹⁶ consisted of two arms placed in contact with the specimen in a conventional triaxial apparatus. The two arms were supported on two posts which passed through the base of the triaxial cell and were connected to an LVDT. Any lateral movement in the soil specimen during the test would cause the arms to rotate, which in turn was measured by the LVDT. The LVDT was monitored with a voltmeter, while an air pressure regulator was adjusted manually to keep the voltmeter as close as possible to the null value during the test. This swinging arms concept was adopted by WES, and a new triaxial cell equipped with this nulling device was constructed for comparative study of K_0 in this report. The major advantage of the swinging arm K_0 device is that the LVDT is placed outside the triaxial cell, which eliminates the influence of confining fluid on the nulling device used in the test.

20. Miscellaneous methods. A very interesting method for testing soil under K_0 conditions was devised at Imperial College.¹⁷ The apparatus used is similar to the conventional triaxial apparatus with the exception that an inner cell surrounding the specimen (see Figure 8) was

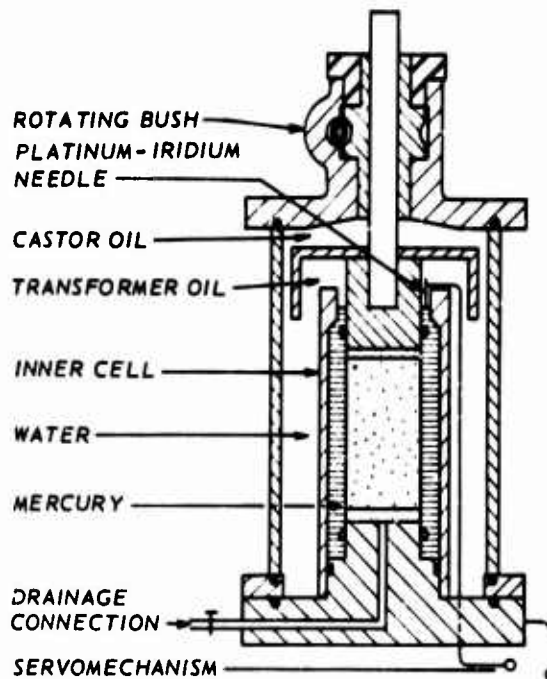


Figure 8. Cell for consolidation with zero lateral yield (diagrammatic) (courtesy of University of Toronto Press and Professor A. W. Bishop¹⁷)

added to the apparatus. The annular space between the inner cell and the specimen was filled with mercury, and a K_0 condition was assumed to be maintained when the level of mercury remained constant during the test. To assure that this level was maintained, a platinum-iridium needle connected to a servomechanism which controlled the axial load was placed in contact with the mercury surface. Departure from the K_0 condition broke the contact between the needle and mercury surface. The axial load was in turn prevented from increasing by a servomechanism controlling the application of cell pressure during K_0 consolidation in this device. The apparatus was used to consolidate soils to cell pressures as high as 1000 psi.

21. Another one-dimensional compression apparatus was designed at the Swedish Geotechnical Institute by Kjellman and Jakobson¹⁸ to test cylindrical specimens of granular material 50 cm in diameter and 100 cm high. The granular material was placed inside a series of steel rings 5 cm high and 0.7 cm thick as shown in Figure 9. These rings were

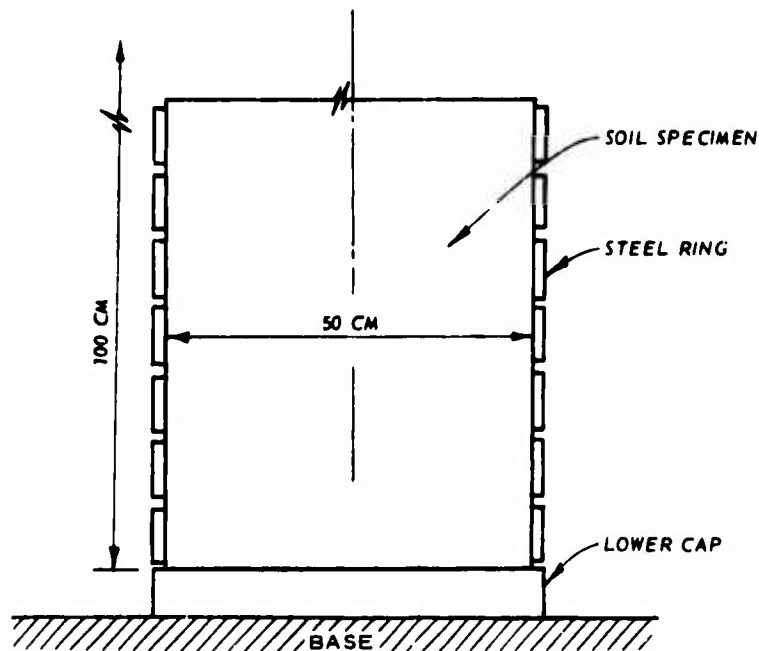


Figure 9. Kjellman and Jakobson apparatus

separated by small gaps which allowed axial strain to occur without developing significant shear stress due to friction. Lateral deformations resulting from the elastic extension of selected rings were measured by mechanical as well as electrical means. The lateral stresses occurring within the soil were calculated, using elastic theory, from the measurement of the lateral deformations of selected rings. Tests conducted on rounded gravel and crushed stones indicated that K_0 during loading was nearly constant with little or no influence by the placement density. The apparatus suffers from the disadvantage that the measurement of K_0 value depended on the amount of lateral yielding that took place during the test; this yielding, no matter how small, is a violation of the K_0 condition.

Use of Bison coils as nulling device

22. A soil strain measuring device manufactured commercially by Bison Instruments was used for measuring and controlling the radial deformation in a series of triaxial compression tests on clay by Gilbert and Townsend.¹⁹ They are available in several types and sizes. The device used by Gilbert and Townsend consisted of two parts. The first

part was composed of two identical circular disks $1\frac{1}{8}$ in. in diameter and $\frac{1}{8}$ in. thick enclosing a circular coil that could generate an electromagnetic field when excited by an electric current. These two disks are usually connected to form an inductance bridge. The second part consisted of an external instrument package which included an amplifier, balancing unit, and readout system. More technical details on the Bison gages can be found in the manufacturer's manual.²⁰

23. In their testing program, Gilbert and Townsend¹⁹ placed the Bison coils parallel to each other on the opposite sides of a triaxial compression specimen, as shown in Figure 10. By observing the change in the output voltage of the unbalanced bridge, they were able to maintain a null condition by adjusting the cell pressure or measuring the radial deformation from a calibration curve. The major advantage of the Bison

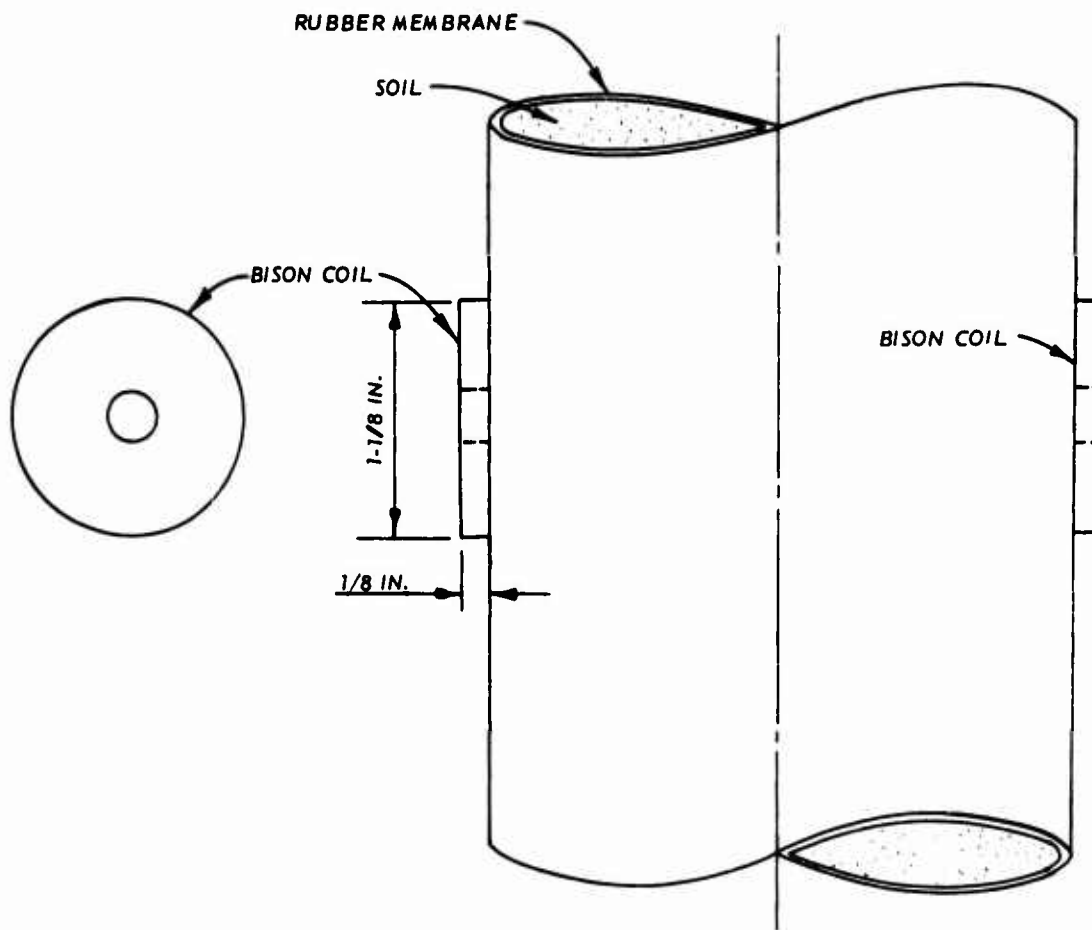


Figure 10. Bison coils mounted on cylindrical soil specimen

coil is that it is battery-operated, thus providing flexibility for use both in the laboratory as well as in the field. The effects of rotational or transverse movement, moisture, and temperature are of little significance. However, because the Bison coils are extremely sensitive to the surrounding metallic objects within their electromagnetic field, they require very complex and time-consuming calibration when used in a metallic triaxial device. They are therefore impractical for routine laboratory testing.

Use of cantilever
spring arm as nulling device

24. Another lateral deformation sensor, called a deformer, was constructed at the Georgia Institute of Technology and used by Mazanti and Holland²¹ both as a nulling indicator for uniaxial strain tests as well as for measuring the radial deformation of specimens during shear. The deformer as shown in Figure 11 consisted basically of three cantilever metal strips placed 120 deg apart with their free ends bearing against the soil specimen at midheight while the opposite ends were fixed to a metal ring attached to a triaxial cell base. The cantilever metal strips were instrumented with electric resistance strain gages for detecting any radial movement of the specimen during the test. The lateral deformer is easy to install, allows in-place calibration, and exerts only an insignificant force on the soil specimen. One disadvantage of the deformer is that points of contact with the specimen are continuously changed as the specimen length changes during the test. Several deformers can be arranged at different elevations around the soil specimen so that a radial deformation profile can be obtained. Multiple deformers stacked around the specimen have been used by Ehrgott²² at WES to obtain the uniaxial stress-strain relationship for undrained soils under static as well as dynamic loading conditions.

Field Measurement of K_o

25. The lateral stresser that develops in remolded soils such as fills may be measured directly by installing pressure cells during

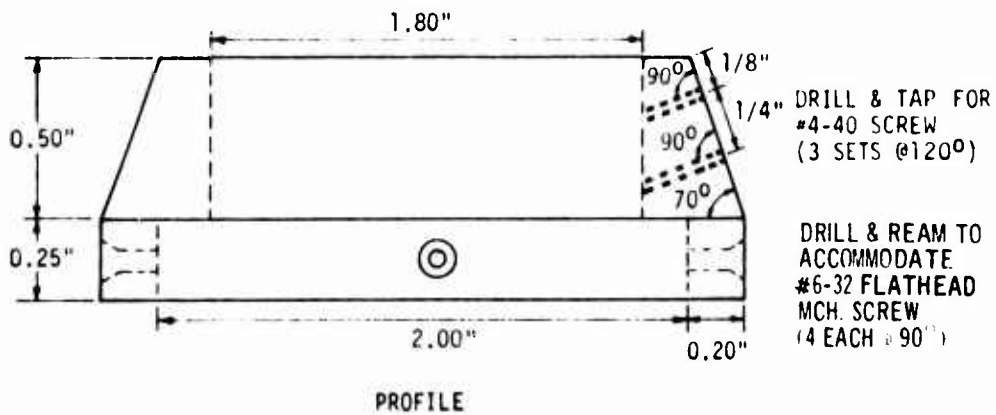
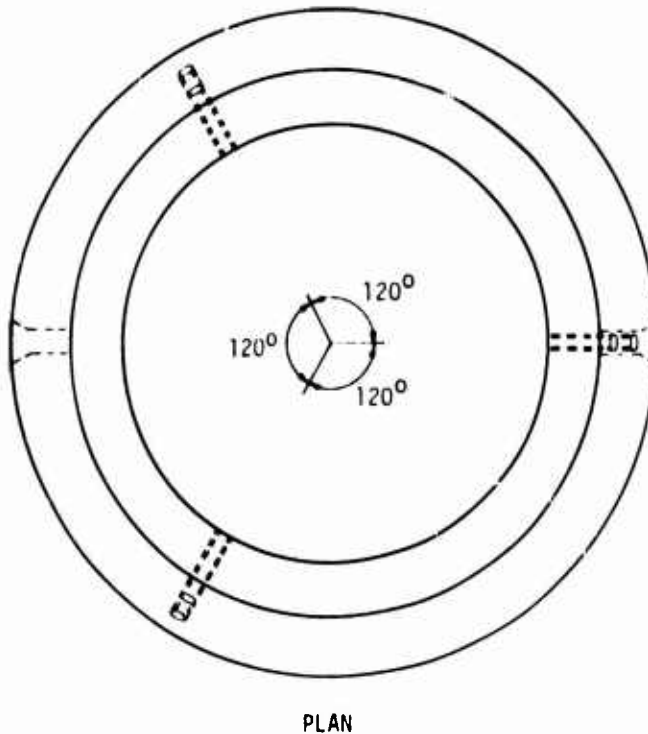
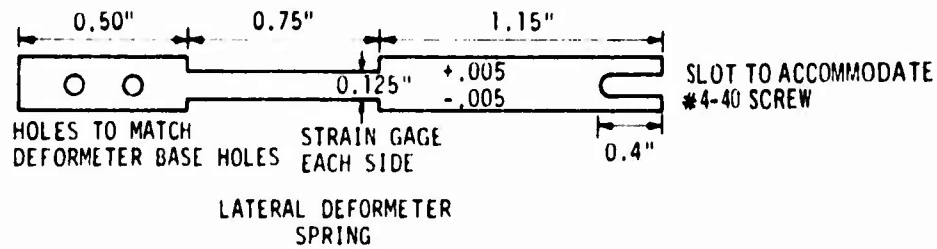


Figure 11. Georgia Institute of Technology lateral deformer (from Reference 21)

construction of the fill; however, exact measurements of the stresses are not easily obtained with the pressure cells. Accurate measurement of lateral stresses in an undisturbed soil is extremely difficult since insertion of any measuring device will cause some disturbance of the soil which adversely affects the local stresses. However, if extra care is taken during installation of the measuring devices and a certain margin of error can be accepted, lateral stresses could be measured in an undisturbed soil with reasonable degree of confidence. Several methods are known to be used for measuring the in situ value of K_0 . A description of some of these methods follows.

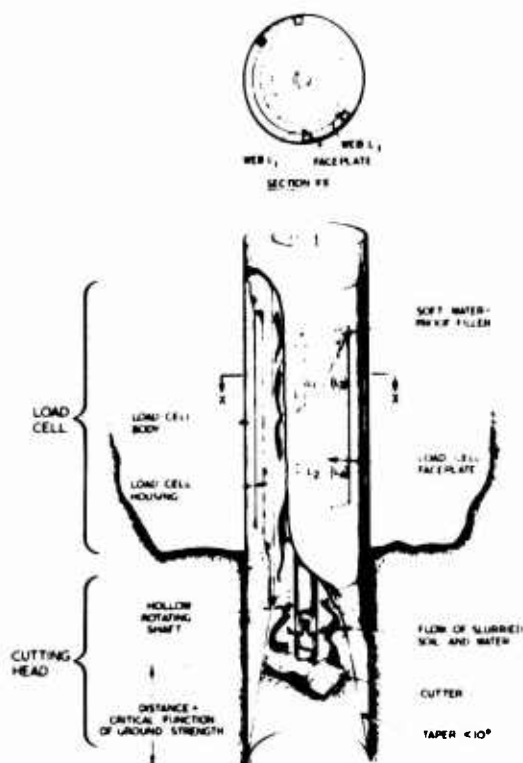
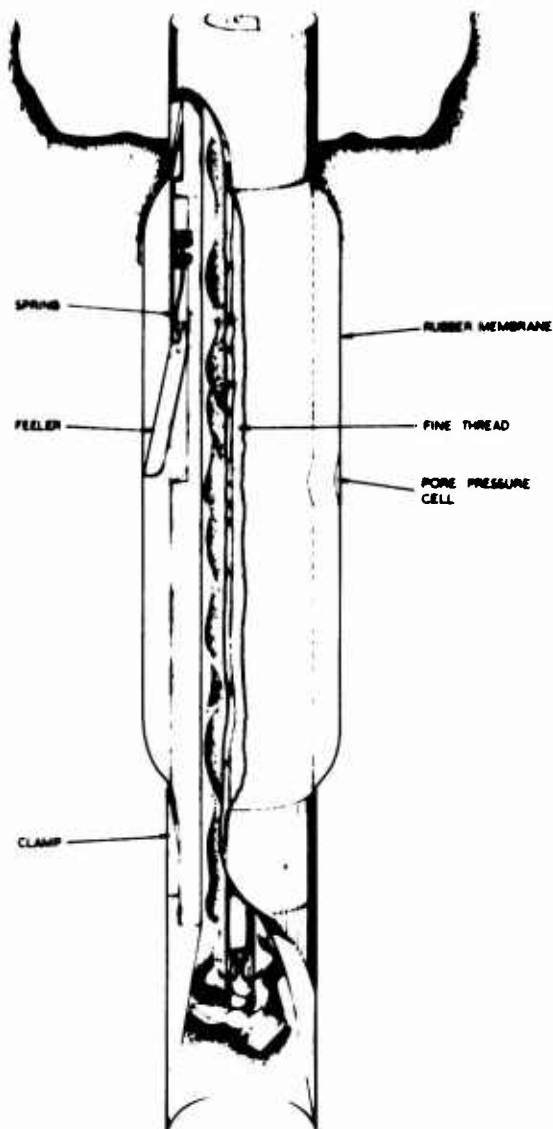
Direct installation
of pressure cells test

26. A special instrument that drilled itself into the ground and measured the lateral stresses was developed at Cambridge University.²³ The instrument shown in Figure 12 consisted of a hollow cylinder which could be pushed slowly into the ground while the soil was being excavated by a rotating cutter. Water circulated down the central tube on which the cutter was mounted and moved upward through the annulus carrying the soil cuttings. The shield which protected the cutter and the rotating shaft was instrumented with pressure cells for measuring the total lateral stress. From the measurements of the lateral stress and calculated axial stress at any depth, the in situ K_0 value could be determined. The top of the instrument was provided with openings which permitted expansion of a rubber membrane against the wall of the bore, thus enabling the measurement of the in situ stress-strain properties of the soil. A series of radiograph pictures taken before and after a controlled test showed that disturbance was confined to a thin zone probably not greater than 2 mm thick from the surface of the instrument. The instrument has been used successfully for soft clay in the field,²³ where measured values of K_0 compared closely with those obtained from hydraulic fracture tests. For stiff soils, however, this instrument may not be useful.

Hydraulic fracture test

27. If a mass of soil is subjected to an increasing internal

a. Overall view of instrument



b. Detailed view of instrument

Figure 12. Field K_0 instrument developed by Cambridge University (courtesy of Professor C. P. Wroth)

pressure, a local fracture in the soil will eventually occur, provided the soil mass has a reasonably low permeability. This simple principle has been used as a basis for calculating the in situ K_0 for normally consolidated soil by assuming that the measured pressure applied to close the local fracture is equivalent to the in situ lateral stress. Tests of this kind have been used by many investigators²⁴⁻²⁶ because of its simplicity and low cost.

28. The hydraulic fracture testing apparatus as described by Bjerrum and Anderson²⁴ (see Figure 13) consists of a piezometer with an

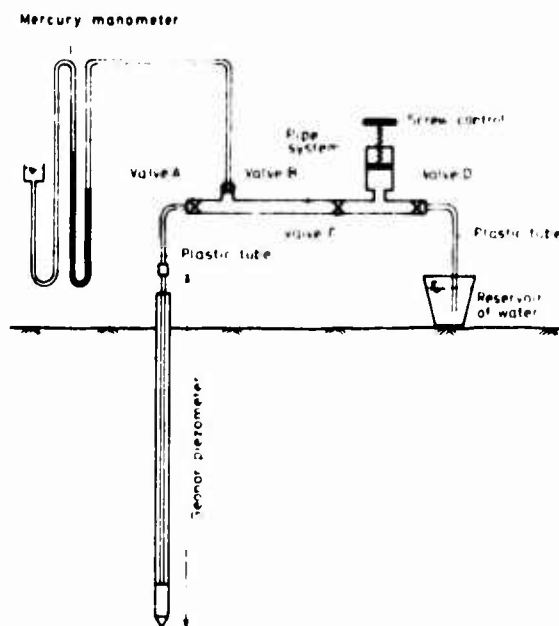


Figure 13. Sketch of the field hydraulic fracture apparatus (courtesy of Sociedad Española de Mecánica del Suelo Cimentaciones²⁴)

outer rod and tip that can be forced into the ground, a control screw for applying pressures, and a mercury manometer for measuring the applied pressures. The piezometer is usually left in the ground for several days after being installed at the desired depth to allow the water level to reach equilibrium and the disturbed zone surrounding the piezometer to consolidate. The test is performed after the system is deaired by forcing water out of the control screw at an increasing rate of flow until cracking of soil occurs. As the pressure approaches a

constant value, the flow of water is stopped and the system is allowed to operate as a falling head permeability test. A plot of the applied pressure versus the rate of flow is then generated, and point of maximum curvature is established. The pressure which corresponds to the maximum curvature is assumed to be equal to the in situ lateral stresses. When the lateral stress and the overburden pressure are known, the value of the in situ K_0 can be determined. Field measurement of K_0 using this method on different kinds of normally consolidated clays compared favorably with those obtained from laboratory measurements.

29. Although the performance of the hydraulic fracture test is simple, the interpretation of the result is difficult since it involves many assumptions concerning the orientation of principal stresses, fracture mechanism, the extent to which seepage pressure develops, and also the shear and tensile strength of the material tested. The test is useful only for a radially symmetric stress system and for normally consolidated or slightly overconsolidated soils where K_0 is less than unity.

Field vibratory test

30. The in situ measurement of K_0 can be obtained indirectly from the measurement of the time required for an elastic wave to travel a known distance within a soil media. The test procedure used by WES²⁷ involves measuring the velocity of waves propagated at known frequencies along the exposed surface of soil (surface or Rayleigh waves) as well as measuring the velocity of waves refracted at known frequencies from a known depth of the soil (compression wave). It has been indicated²⁸ (see Figure 14) that the difference between the surface wave and the shear wave with the change in Poisson's ratio is so small that the propagated surface waves can be considered as shear waves for all practical purposes.

31. For isotropic elastic media the shear wave velocity V_s and the compression wave velocity V_c may be expressed as

$$V_s = \left(\frac{G}{\gamma} \right)^{1/2} \quad (1a)$$

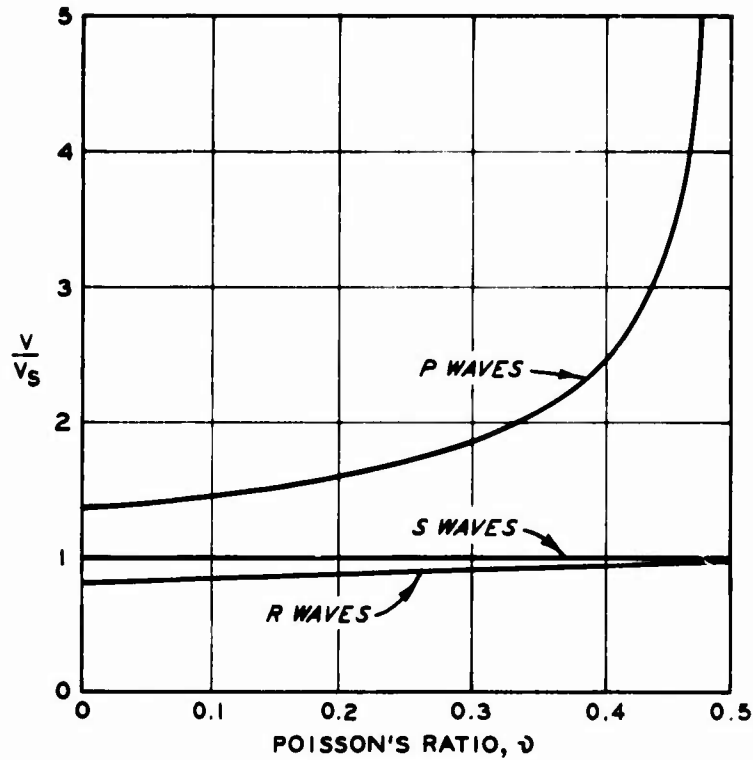


Figure 14. Relation between Poisson's ratio ν and velocities of propagation of compression (P), shear (S), and Rayleigh (R) waves in a semi-infinite elastic medium (from Reference 28)

$$v_c = \left(\frac{Eg}{\gamma} \right)^{1/2} \quad (1b)$$

where

G = shear modulus

g = gravity acceleration

γ = in situ unit weight of soil

E = elastic modulus

When the shear wave and compression wave velocities of the soil media are known, the value of Poisson's ratio ν and K_o can be calculated as

$$\nu = \frac{1 - \left(\frac{v_s}{v_c} \right)^2}{2 - 2 \left(\frac{v_s}{v_c} \right)^2} \quad (2a)$$

$$K_o = 1 - 2 \left(\frac{v_s}{v_c} \right)^2 \quad (2b)$$

32. The major advantage of the vibratory field test is that a considerably large area can be tested quickly without disturbing the soil. Also the theoretical basis of the method is sound and simple. However, the disadvantage of the method is that the soil media is assumed to be isotropic and elastic, thus the values of v and K_o represent more or less average values for all the material encountered in the site tested.

Theoretical Evaluation of K_o

33. Although there are many procedures for determining the value of K_o by experimental means, there have been only two successful attempts for predicting K_o analytically. The first theoretical approach was derived by Jaky²⁹ and the second was derived by Hendron.⁶

Jaky theory

34. Jaky²⁹ postulated that a semi-infinite granular mass can be divided into two major zones as shown in Figure 15. The first zone is

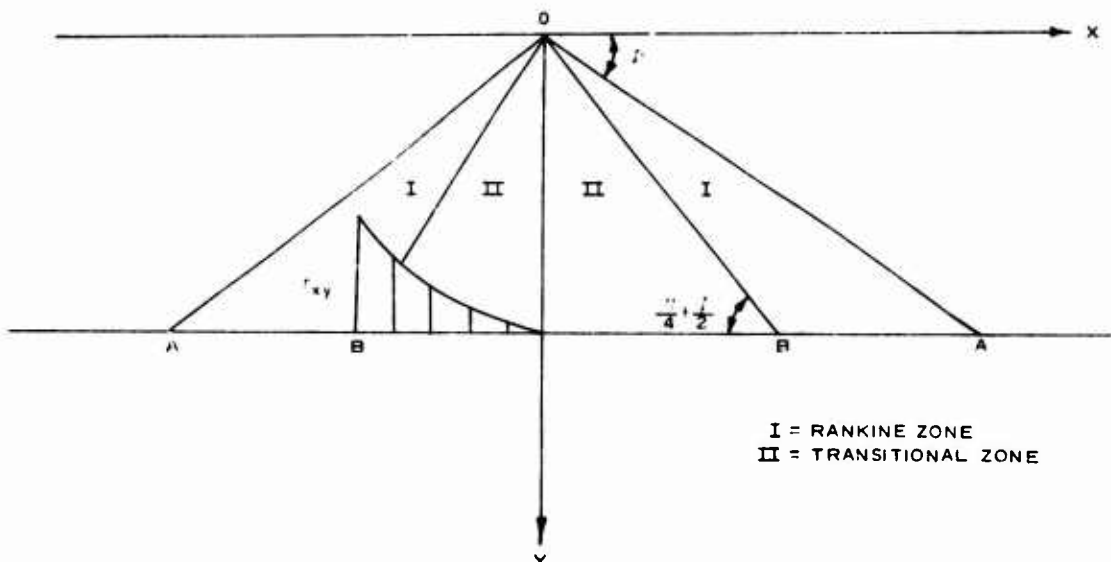


Figure 15. Rankine and transitional zones as assumed by Jaky²⁹

the Rankine zone (I) bounded by lines at angles of ϕ and $(\pi/4 + \phi/2)$ with the horizontal plane, where ϕ is the failure angle. The second zone (II) is a transitional zone extending from OB which represents the limiting equilibrium boundary to OY which represents the elastic state. Jaky also assumed that the shear distribution on any horizontal plane within the transitional zone is parabolic. Using equilibrium conditions and Rankine theory, Jaky was able to derive an expression for K_o as follows:

$$K_o = \left(1 + \frac{2}{3} \sin \phi\right) \tan^2 \left(\frac{\pi}{4} - \frac{\phi}{2}\right) \quad (3)$$

The value of ϕ for typical soils ranges from 20-45 deg, and without significant loss of accuracy, Equation 3 may be simplified further to

$$K_o \approx 0.9(1 - \sin \phi) \quad (4)$$

However, if the shear distribution were chosen to be cubic rather than parabolic, the 0.9 would have been slightly greater than 1.0. Thus a good approximation for K_o would be

$$K_o \approx (1 - \sin \phi) \quad (5)$$

Hendron theory

35. The theoretical derivation of Hendron⁶ is based on the assumption that a uniform, well rounded, dense sand can be approximated by a face-centered array of equiradii spheres as shown in Figure 16. Hendron showed that if the array of spheres was subjected to one-dimensional compression, then the value of K_o , which he defined as the ratio of vertical to horizontal force, can be expressed as

$$K_o = \frac{1}{2} \left(\frac{1 - f}{1 + f} \right) \quad (6)$$

where f is the coefficient of friction at point of contact between spheres.

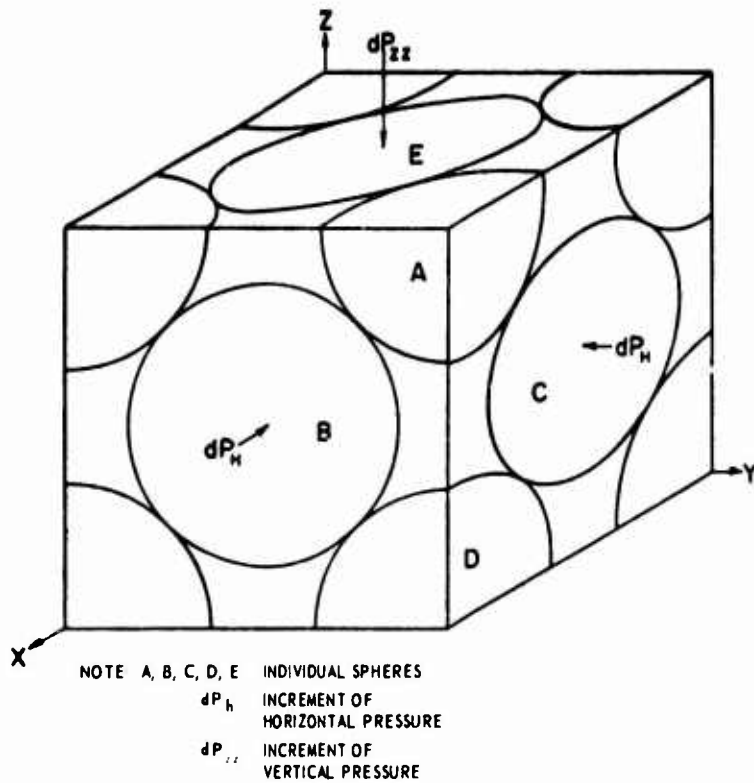


Figure 16. Unit cube of a face-centered cubic array of equal spheres subjected to incremental forces in one-dimensional compression (after Hendron⁶)

36. Hendron also showed that the ratio of the minor to the major principal stresses can be expressed in terms of the coefficient of friction f as

$$\frac{\sigma_3}{\sigma_1} = \frac{\sqrt{6} - 4f}{2(\sqrt{6} + 2f)} \quad (7)$$

where σ_1 is the major principal stress and σ_3 is the minor principal stress. Because it is difficult to determine f for particles with small diameter, Hendron used the failure condition to solve for the coefficient of friction f . The ratio of principal stresses at failure for dry granular material is defined by

$$\frac{\sigma_3}{\sigma_1} = \frac{1 - \sin \phi}{1 + \sin \phi} \quad (8)$$

Equating Equations 7 and 8, the coefficient of friction can be expressed in terms of $\sin \phi$ as

$$r = \frac{3\sqrt{6}}{8} \sin \phi - \frac{\sqrt{6}}{8} \quad (9)$$

Consequently the coefficient of earth pressure at rest and the angle of internal friction for a face-centered array can be related to each other by combining Equations 6 and 9 in the following form:

$$K_o = \frac{1}{2} \left[\frac{1 + \frac{\sqrt{6}}{8} - 3\left(\frac{\sqrt{6}}{8}\right) \sin \phi}{1 - \frac{\sqrt{6}}{8} + 3\left(\frac{\sqrt{6}}{8}\right) \sin \phi} \right] \quad (10)$$

The relationship between K_o and $\sin \phi$ as suggested by Jaky and Hendron is shown in Figure 17. It can be seen that the two expressions diverge quantitatively, but their trend is similar in the qualitative sense. It must be noted that the majority of experimental data on well rounded cohesionless soils tend to confirm Hendron's theory, while experimental data on cohesive soils as well as on cohesionless soils with angular particles agree more closely with Jaky's theory.

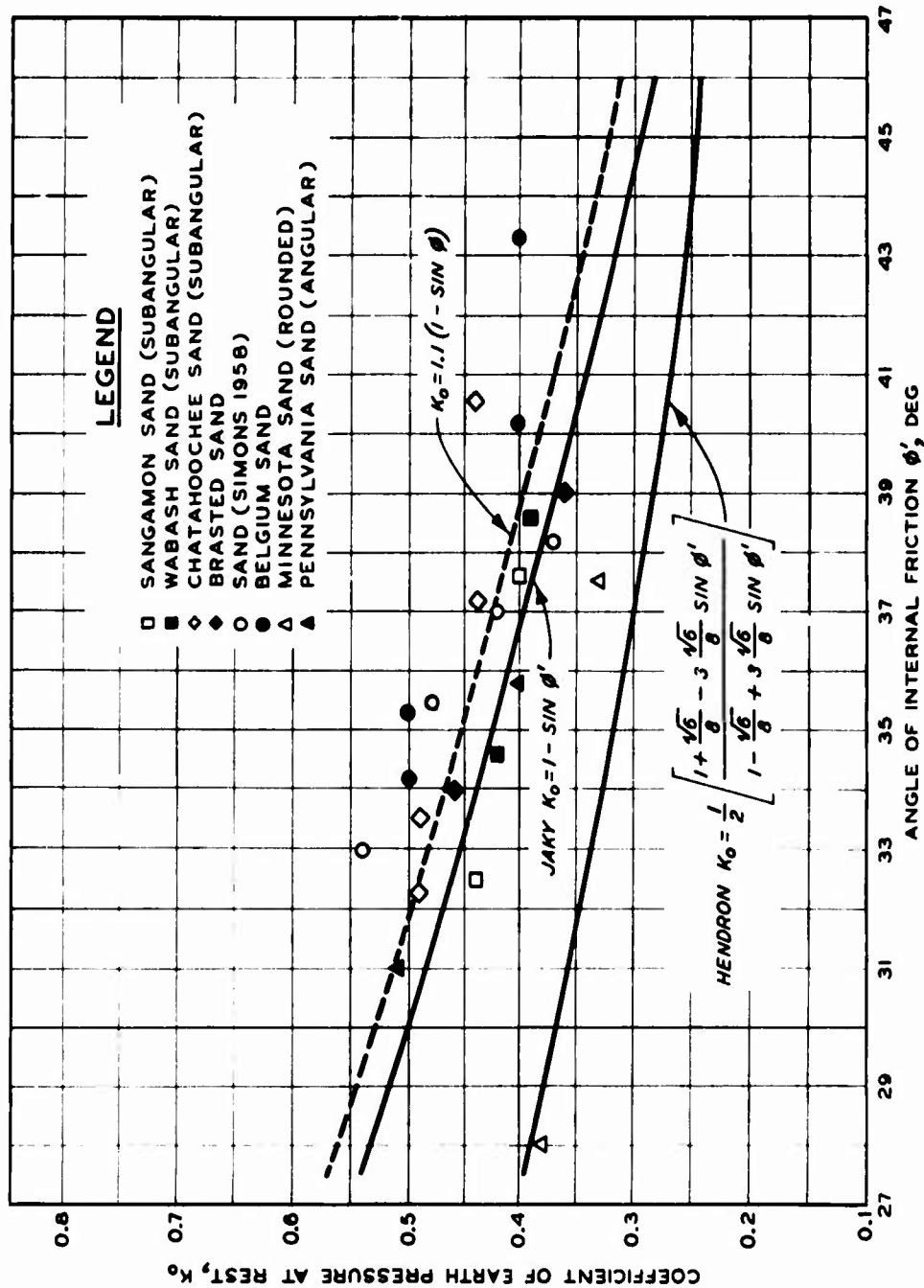


Figure 17. Relationship between K_0 and ϕ' for different cohesionless materials (from Reference 30)

PART III: MATERIAL, TESTING EQUIPMENT, AND PROCEDURES

Material

37. The Reid-Bedford sand used in the test program was originally obtained from the Campbell swamp area along the Mississippi River about 15 miles south of Vicksburg, Mississippi. It is a uniform sand as shown in Figure 18 with a grain shape varying from subrounded to sub-angular and a very small amount of material finer than the No. 200 U. S. standard sieve. Other physical properties of the Reid-Bedford sand are given as follows:

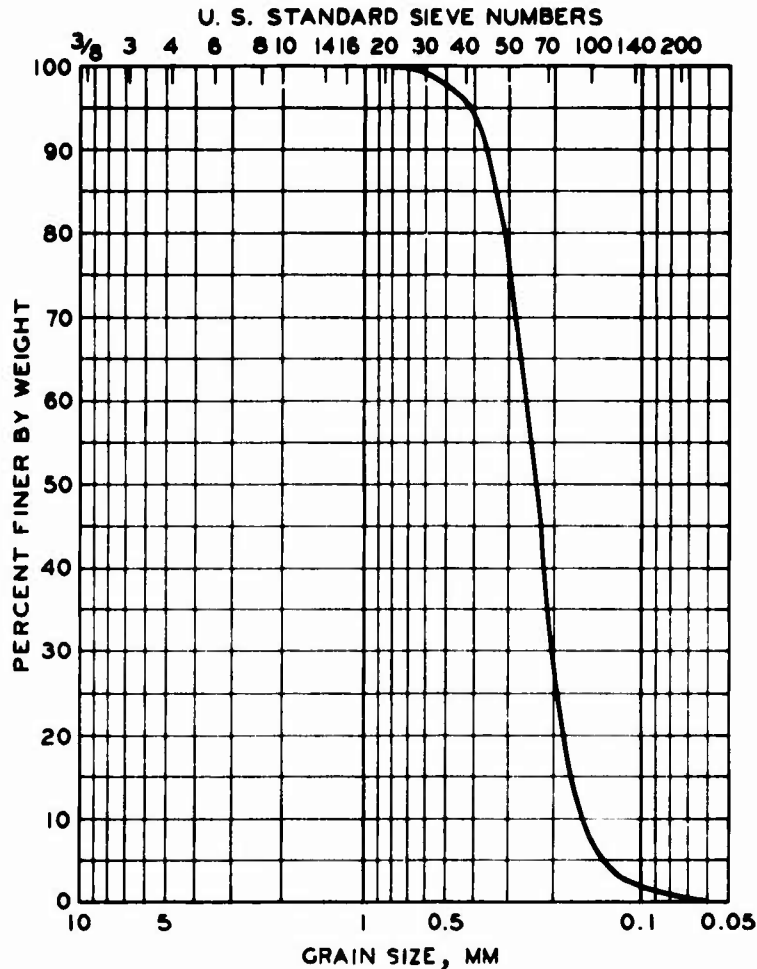


Figure 18. Gradation curve for Reid-Bedford sand

Specific gravity, G_s	2.66
Maximum void ratio, e_{max}	0.903
Minimum void ratio, e_{min}	0.593
Mean grain diameter, D_{mean}	0.125 mm
Coefficient of uniformity, C_u	1.5
Unified Soil Classification	(SP)

Testing Equipment

38. The main testing equipment used in the test program was a conventional triaxial apparatus with enlarged low friction cap and base similar to the one shown in Figure 19. However, four different methods for sensing the lateral deformation of the specimen during the K_o test were employed.

LVDT clamp lateral strain sensor

39. The lateral strain sensor shown in Figure 20 consisted of two 3/16-in.-thick curved aluminum strips connected by a low friction hinge. A soft steel spring at the other end provided tension for holding the clamp bearing surface snugly against the specimen. A small amount of rubber cement between the bearing surfaces and specimen membrane assisted in holding the clamp in position. The geometry of the lateral strain sensor and position of the LVDT were such that the sensor indicated radial deformations which were twice the actual radial deformations of the soil specimen. After the soil was prepared at the desired density, the lateral strain sensor was placed horizontally around the midheight of the specimen as shown in Figure 21.

Strain-gaged K_o belt

40. This lateral strain sensor, called the K_o belt, has been fully described in a previous study;¹² the description herein is limited to the essential parts. The K_o belt consists of a thin brass alloy band welded to a short piece of hose clamp with an adjustable thumbscrew. The two ends of the belt and a small pin form a hinge which can be engaged and disengaged very easily as shown in Figure 22. Four strain gages were mounted on the brass foil band. Two active gages were placed

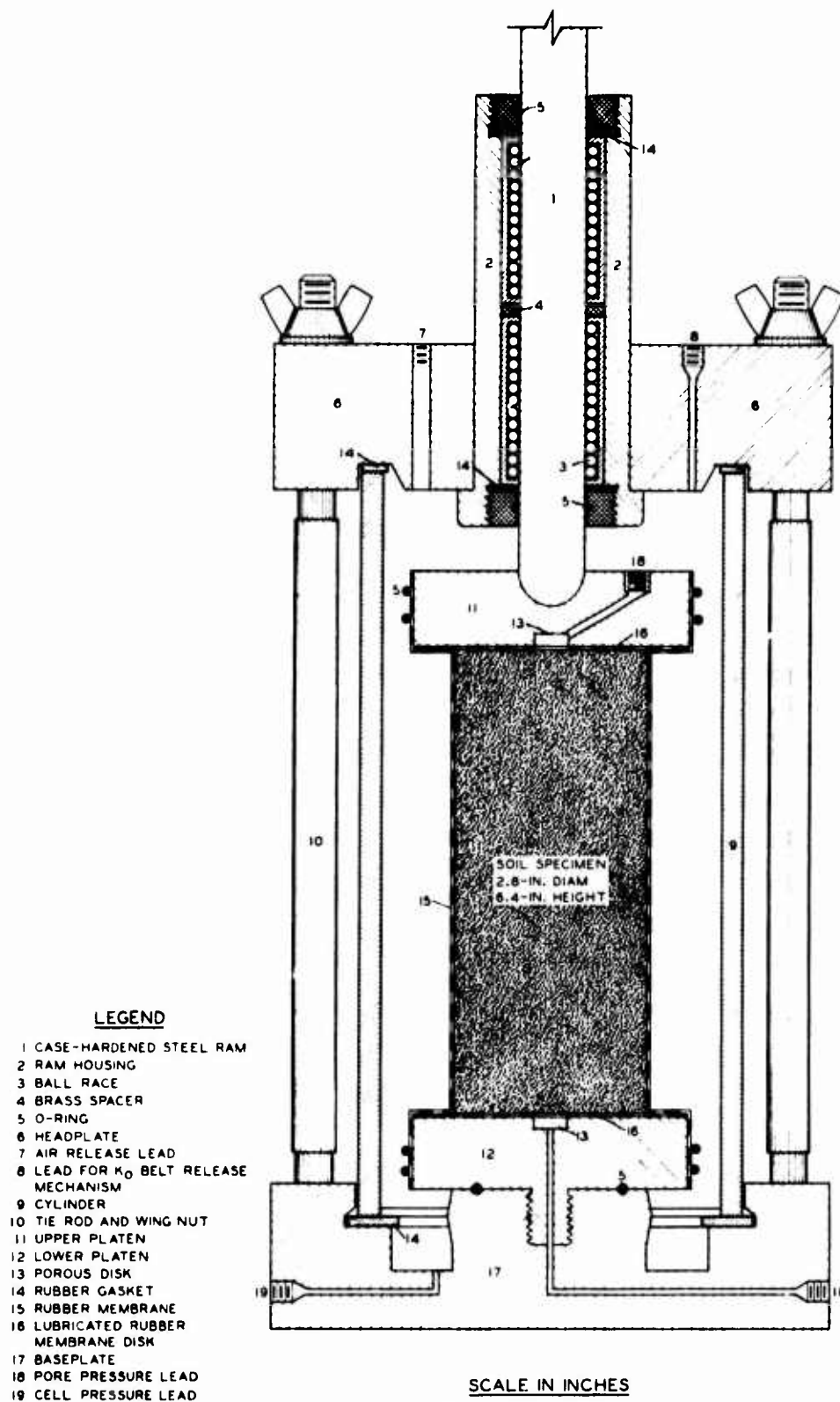


Figure 19. Triaxial apparatus with enlarged low-friction platens (from Reference 31)

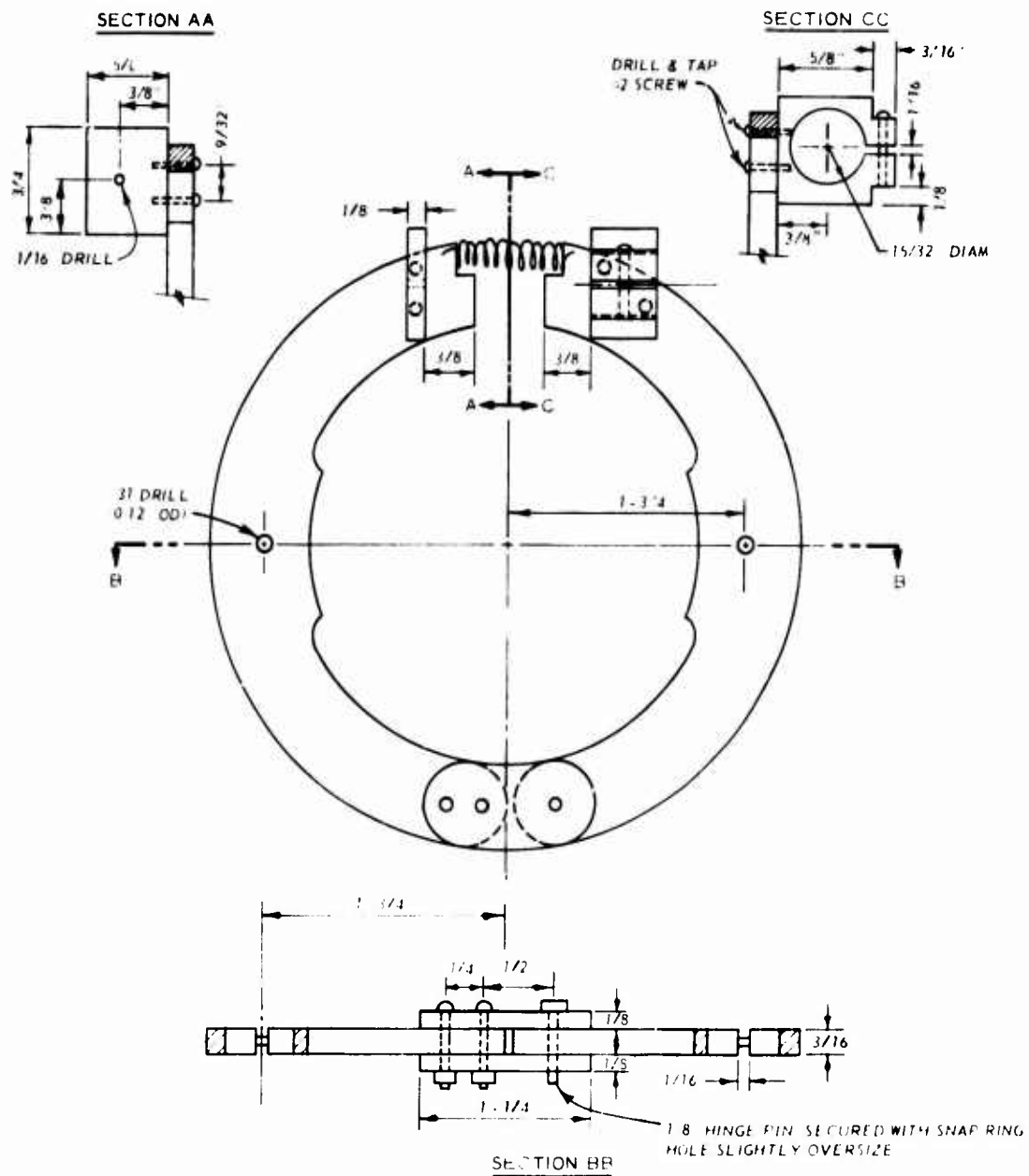


Figure 20. LVDT clamp lateral strain sensor

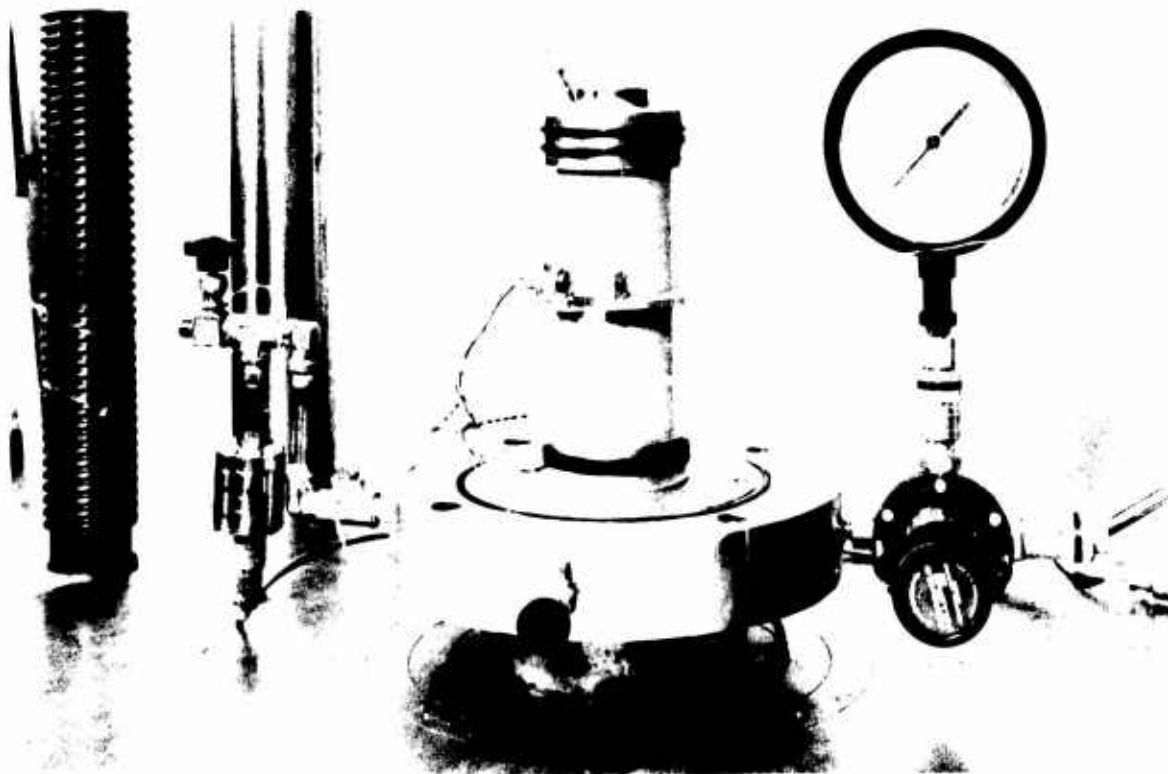


Figure 21. Lateral sensor with LVDT clamp around the specimen

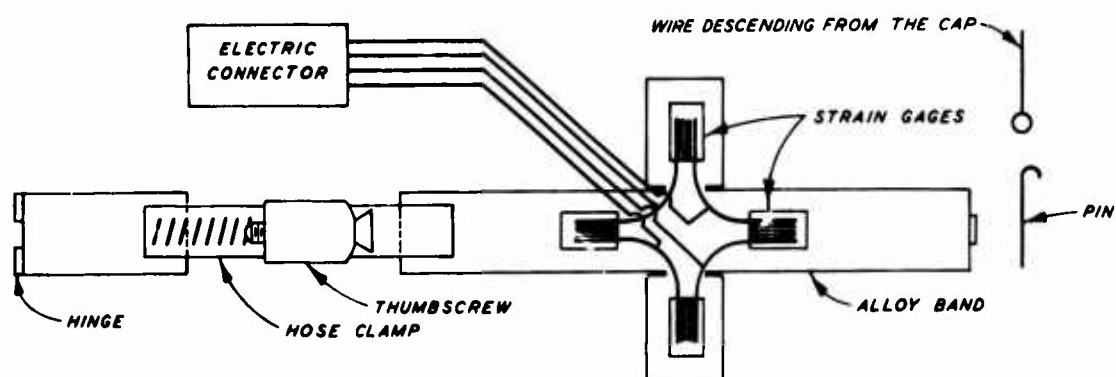


Figure 22. Lateral strain sensor (K_0 belt) (from Reference 12)

along the circumference and the other two were dummy gages placed along the vertical axis on the portion of the band which projected above and below the main band. The sensitivity of the strain gages to applied pressure was found to be approximately equal to 6 μ v for each 100-psi increment of applied load, which was considered an acceptable error. Figure 23 shows the K_0 belt in position on a specimen.

Swinging arms lateral strain sensor

41. This was the only sensing device which required some major modifications in the original triaxial cell presented previously in Figure 19. The lateral sensor with swinging arms as shown schematically in Figure 24 consists of three components: two arms, two posts, and the LVDT holder. Each arm consists of an aluminum plate 4-1/4 in. long, 2.0 in. wide and 1/4 in. thick with a 1/4-in.-diam hole drilled 5/8 in. deep to accommodate the post. A strip of Teflon was glued on the arms to minimize friction between the specimen membrane and arms as the specimen deformed axially during testing. Two identical stainless steel posts were made, each 6-3/4 in. long and 5/16 in. in diameter reduced to 1/4 in. at the ends to facilitate proper fit with other components of the device as shown in Figure 24. The LVDT holder consisted of two aluminum plates, 5 in. long, 1-1/4 in. wide and 1/2 in. thick with one plate to hold the LVDT in position and the other its core.

42. Two modifications were made on the original triaxial cell; the first was to drill two holes in the base to allow the passage of the posts through the magnetic seal and ball race bushings seated within the holes as shown in Figure 24. The second modification was to mount the triaxial cell on four stainless steel foundation posts. Each post was 1.0 in. in diameter and 3.0 in. long threaded at the top to the base of the triaxial cell and connected at the bottom to a square aluminum base plate 8.0 in. wide and 1/2 in. thick. The swinging arms lateral strain sensor is shown in Figure 25. The most outstanding feature of this device is that the LVDT which senses the deformation of the specimen is isolated from any detrimental chamber fluids, whereas the LVDT clamp sensor and the K_0 belt require that air or silicone oil be used as the chamber fluid. The magnetic seal was found to offer

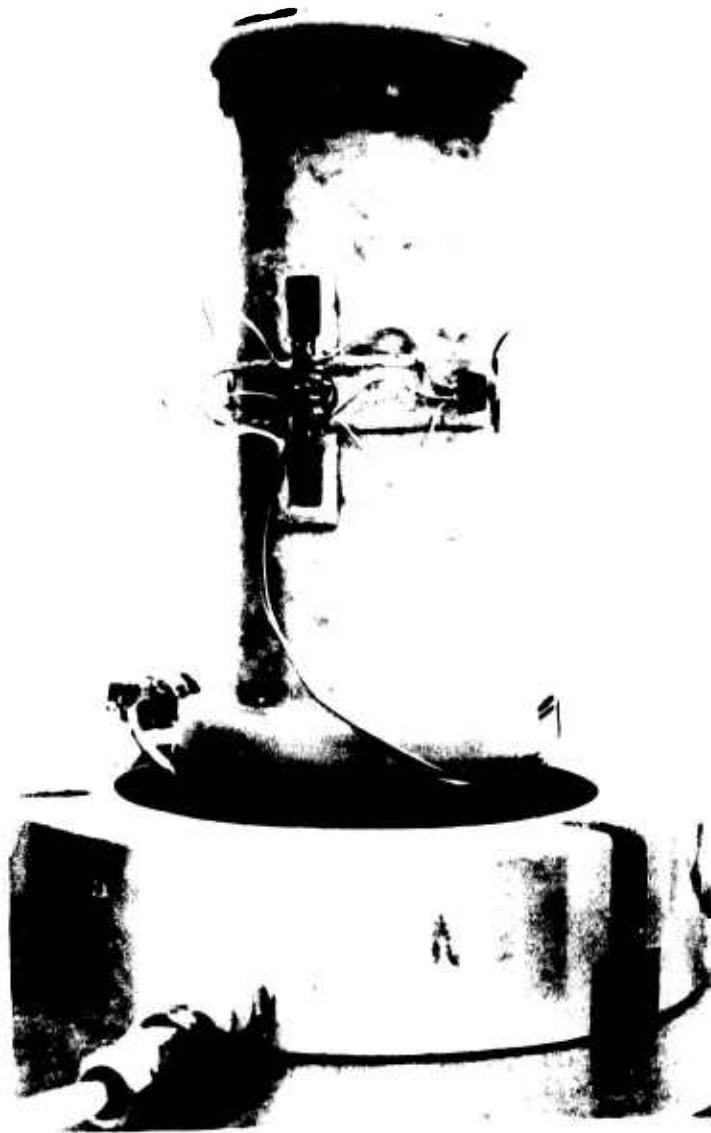


Figure 23. K_o belt mounted on the triaxial specimen

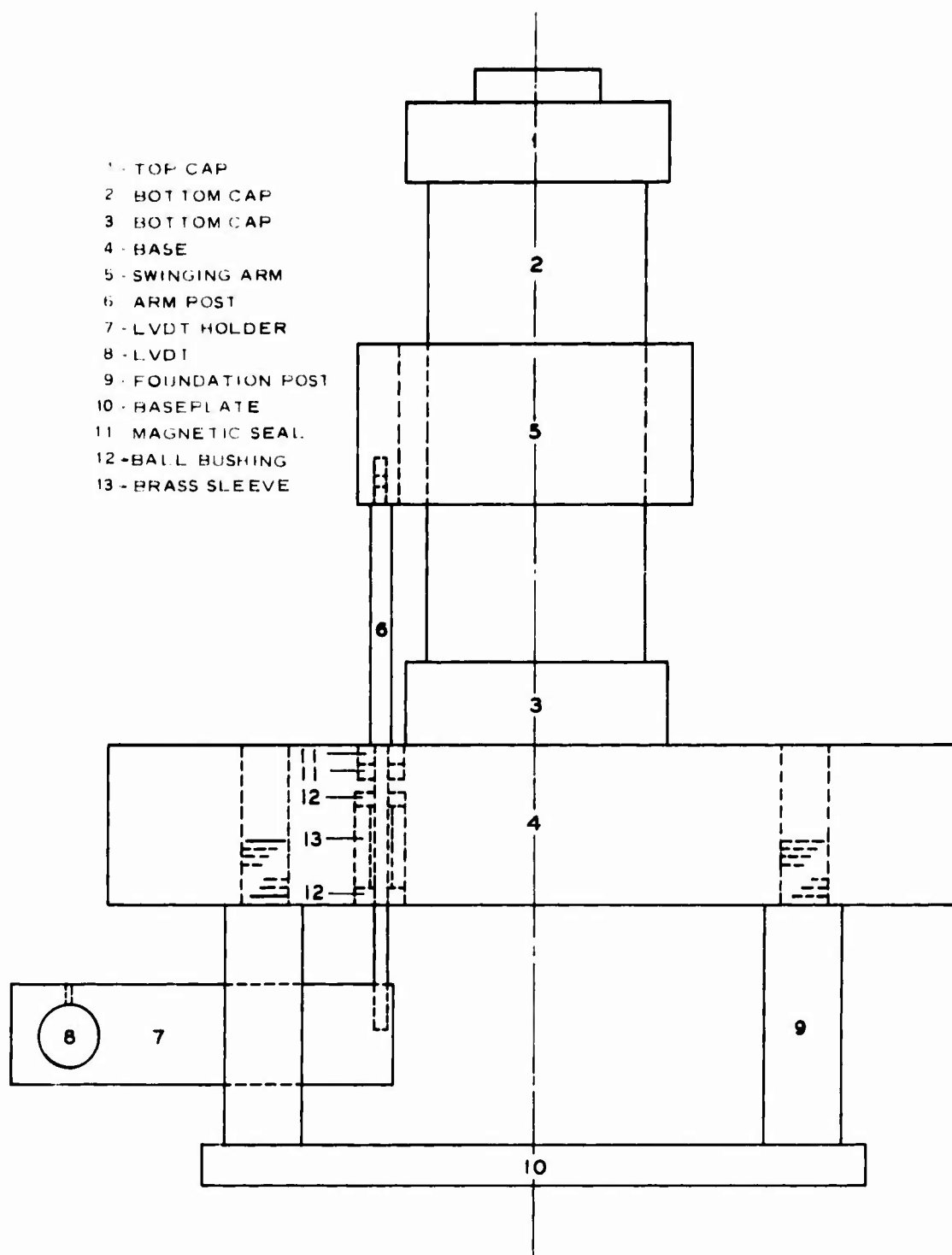


Figure 24. Schematic of lateral strain sensor with swinging arms

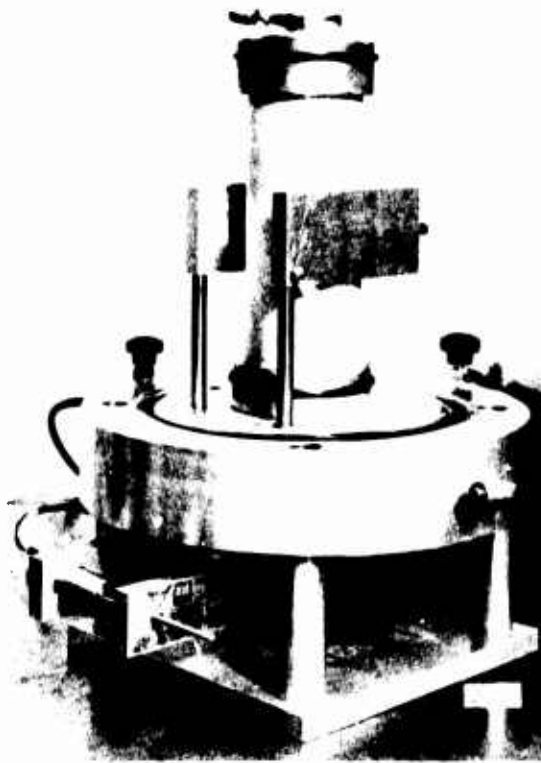


Figure 25. Lateral strain sensor with swinging arms

negligible resistance to the rotation of the post in the horizontal plane; however, any slight tilting of the post from the vertical position could have broken the seal and caused leakage of the chamber fluid.

Indirect or burette method

43. This method did not use a lateral strain sensor, as the volume change of the soil specimen was used to indicate whether or not zero lateral strain conditions were maintained during K_0 tests. The test method and equipment (see Figure 26) were based on the assumption that the volumetric strain of the specimen during one-dimensional compression is equal to the axial strain. In other words, the ratio of the change in volume to the change in height is constant and equal to the initial area of the specimen. Therefore, if the initial area of the soil specimen and the change in height of the specimen are known, it is possible to adjust the cell pressure such that the volume change indicated by the burette is equivalent to the calculated volume change.

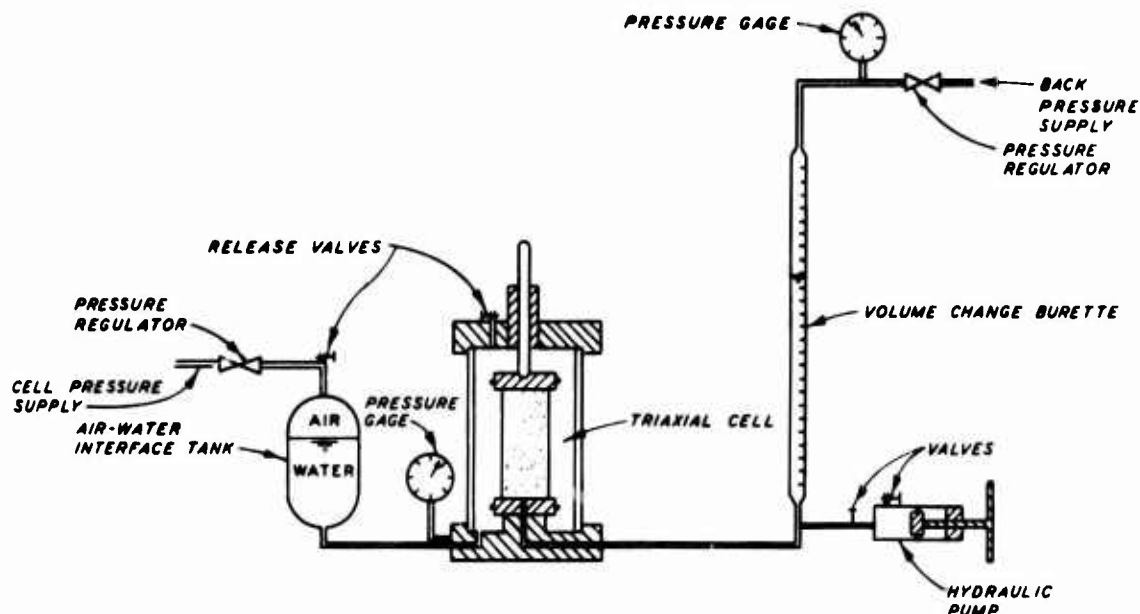


Figure 26. General layout of the hydraulic system (after Reference 30)

This method requires proper correction for membrane penetration and other factors which might influence the observed volume change measurements. The procedure used for determining the effects of membrane penetration consisted of using the LVDT clamp lateral strain sensor with the burette on saturated specimens. The membrane penetration for various pressures was assumed equal to the difference in volume between that calculated using the LVDT clamp deformations and that observed in the burette. By calibrating membrane penetration effects for several densities, membrane penetration corrections could be made for future tests.

Test Procedures

44. All specimens were molded in an air-dried condition inside a 2.8-in.-diam by 6.0-in.-high mold. Desired densities were achieved by vibrating each layer to the proper density with a hand-held air hammer. All specimens except those tested by the burette method were tested dry, while the burette method specimens were saturated by placing

the specimens underwater and subjecting them to a vacuum to remove any air prior to testing.

45. The test procedure used in consolidating the specimen with no lateral yielding was about the same whether the lateral sensor was instrumented with an internal or external LVDT or strain gages. First a null reading was established on the readout system connected to the lateral strain sensor used for the particular test. Both axial load and confining pressure were increased simultaneously such that a null condition was maintained during the entire test. Readings of axial load and axial deformation were recorded at every 10-psi increment of confining pressure.

46. The procedure used in the indirect method was slightly different from the test procedure used in the other methods since no null point was needed in this test. First, a correlation was computed between the change in height and the change in the observed volume of the specimen under no lateral yielding, and then the axial load and cell pressure were increased as dictated by the computed correlation. The procedure was slow and tedious and required continuous adjustment of the cell pressure; readings were taken whenever the collected test data fell on the established volume change versus axial deformation relationship.

PART IV: TEST RESULTS AND DISCUSSION OF EXPERIMENTAL RESULTS

47. During K_o consolidation, the diameter at midheight of the specimen was held constant. The average axial stress σ_a was assumed to be equal to the major principal stress σ_1 , and the radial stress σ_r was considered to be equal to the minor principal stress σ_3 .

48. Generally, the value of K_o for the Reid-Bedford sand was found to be practically the same irrespective of the method used in controlling the radial deformation of the specimen. A special effort was made to present the various factors affecting the value of K_o and to correlate the experimental data with available theoretical analysis. The axial stress behavior for the Reid-Bedford sand tested was found to vary slightly from one method of radial restraining to the other. An explanation and the implication of such variation were offered.

Coefficient of Earth Pressure at Rest K_o

49. The stress-strain curves for the Reid-Bedford sand tested using the LVDT clamp, the swinging arms, the K_o belt with strain gages, and the burette method are shown in Figures 27-30, respectively. The upper portion of these figures shows the relationship between the radial and axial stress, while the bottom portion shows the relationship between the axial stress and axial strain. It is apparent from these graphs that the relationship between σ_r and σ_a can be approximated by a straight line passing through the origin; consequently, K_o can be expressed as the ratio of σ_r to σ_a . Values of K_o for the sand tested using the LVDT clamp, swinging arms, the K_o belt with strain gages, and the burette method are presented in the following tabulation.

LVDT Clamps		Swinging Arms		K_o Belt		Burette Method	
Relative Density	K_o	Relative Density	K_o	Relative Density	K_o	Relative Density	K_o
$D_r, \%$		$D_r, \%$		$D_r, \%$		$D_r, \%$	
30.9	0.53	25.6	0.51	26.9	0.55	36.0	0.52
75.1	0.45	72.1	0.42	72.9	0.48	69.3	0.44
94.0	0.39	99.5	0.39	96.5	0.42	96.8	0.39

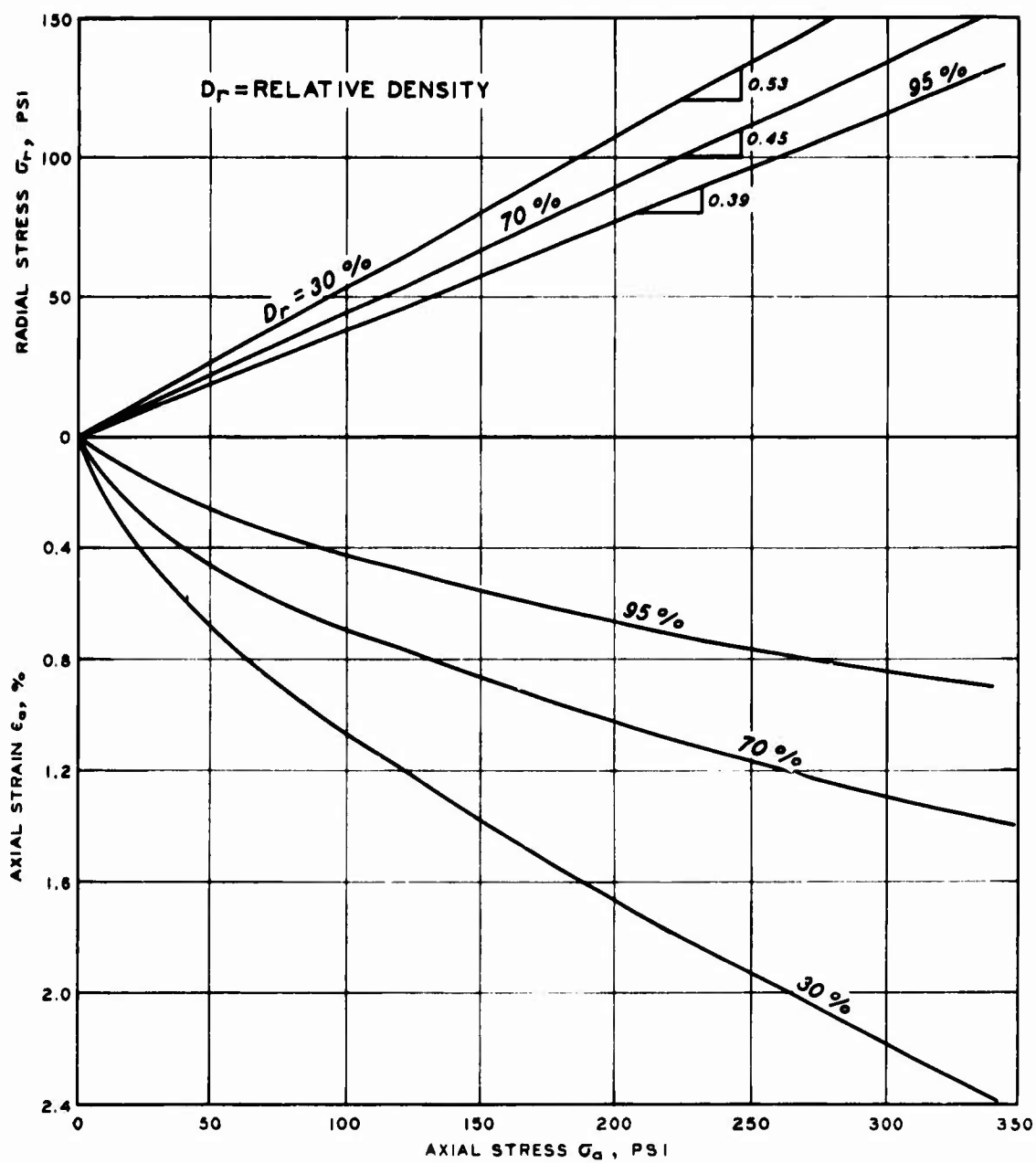


Figure 27. Stress-strain relationship for Reid-Bedford sand under K_0 condition using LVDT clamp

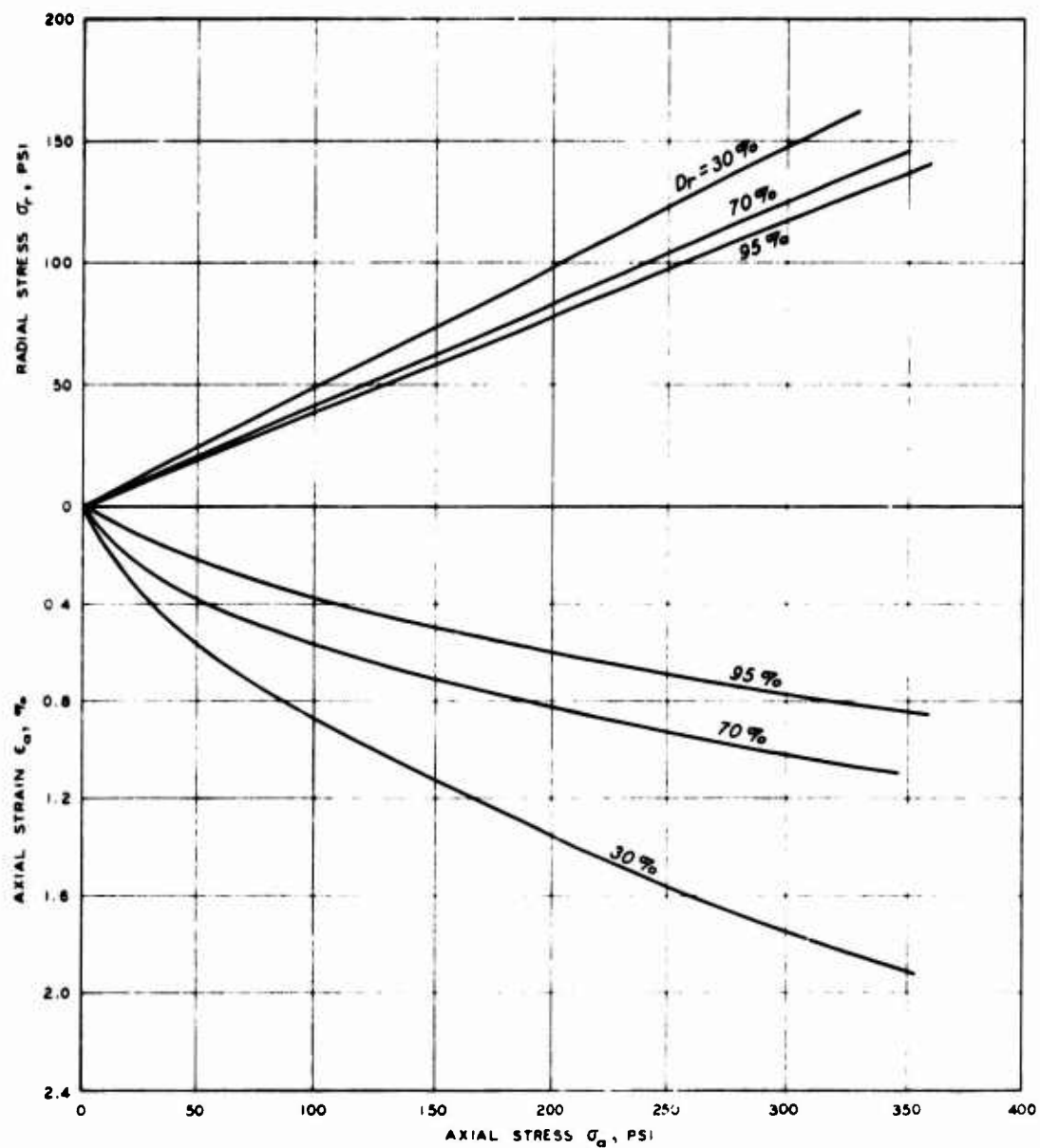


Figure 28. Stress-strain relationships for Reid-Bedford sand under K_0 condition using swing arms

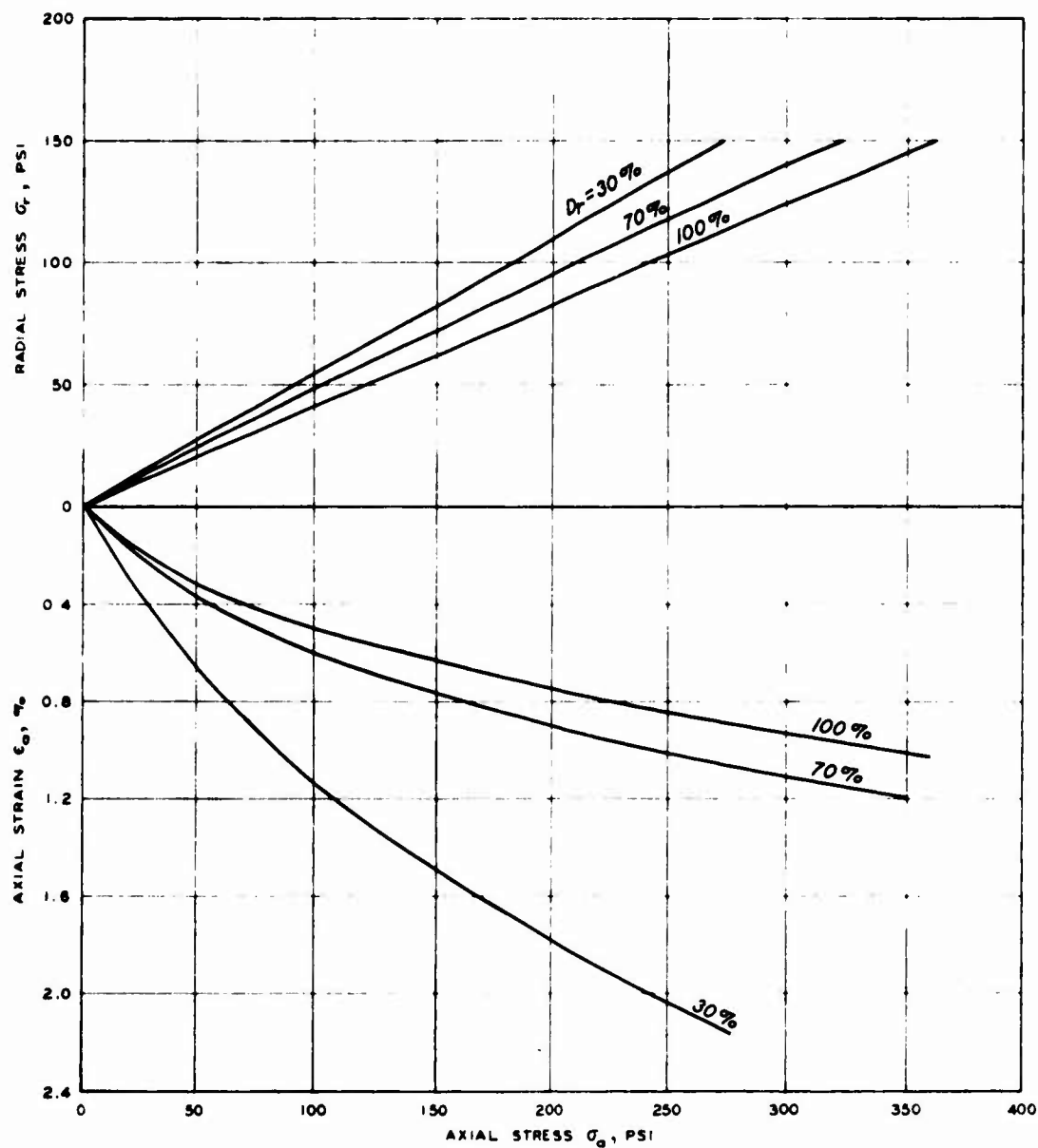


Figure 29. Stress-strain relationships for Reid-Bedford sand under K_0 condition using K_0 belt with strain gages

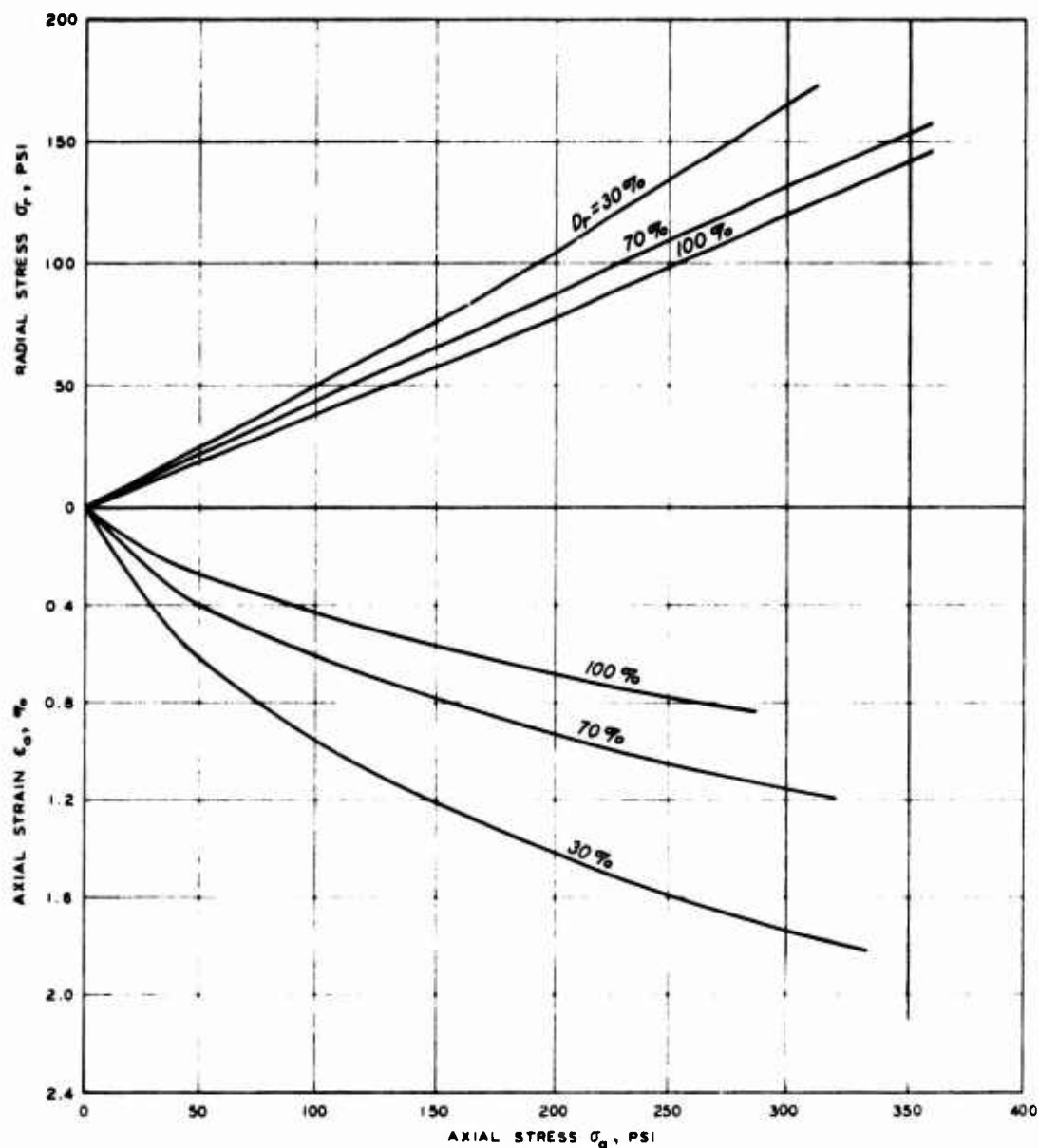


Figure 30. Stress-strain relationships for Reid-Bedford sand under K_0 condition using burette method

This tabulation shows that, at any given sand density, the value of K_0 has the same order of magnitude for all the methods selected in this study for restraining radial deformations. This indicates that all four methods provide the same acceptable degree of accuracy in measuring K_0 and the preference of one method over the others in obtaining K_0 may be a matter of convenience rather than the accuracy of the result. It must be pointed out that the K_0 belt with strain gages tends to give the highest value of K_0 , while the swinging arms sensor tends to yield the lowest. The average value was accepted as the actual value of K_0 for the Reid-Bedford sand. Figure 31 shows that K_0 decreases with increasing relative density.

50. For isotropic elastic materials the value of Poisson's ratio, ν , may be expressed as:

$$\nu = \frac{K_0}{1 + K_0} \quad (11)$$

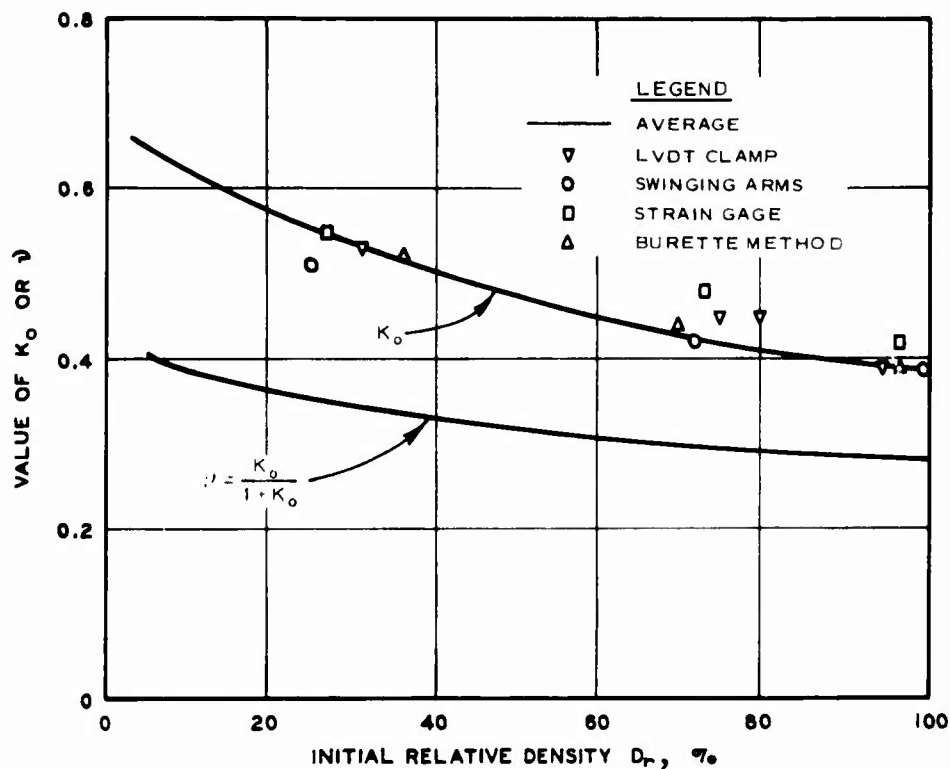


Figure 31. Relationship between K_0 , ν , and D_r for Reid-Bedford sand

The variation of ν as calculated from K_0 with respect to the initial relative density of the Reid-Bedford sand is also presented in Figure 31. The trend of the data was expected because previous investigators such as Jaky²⁹ and Hendron⁶ have reported that K_0 is inversely proportional to the angle of internal friction ϕ .

51. In an effort to verify Jaky's²⁹ and Hendron's⁶ relationships between the angle of internal friction, ϕ , and K_0 , data³² from a series of consolidated-drained direct shear tests were modified to obtain a relationship of ϕ' , the effective angle of internal friction, as a function of relative density, D_r , as shown in Figure 32. The relationship between ϕ' and K_0 was obtained for the Reid-Bedford sand by taking a value of K_0 from Figure 31 corresponding to a given relative density value of ϕ' corresponding to the same relative density from Figure 32. The resulting ϕ' versus K_0 correlation is presented in Figure 33. The experimental results conform closely to the

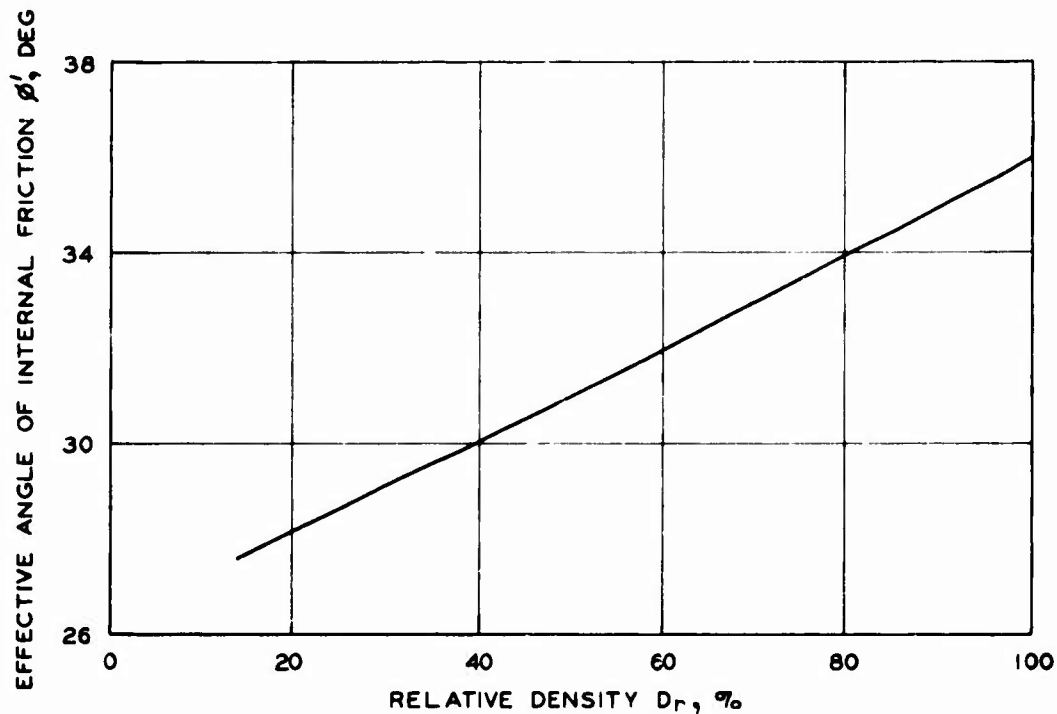


Figure 32. Consolidated-drained direct shear test for Reid-Bedford sand

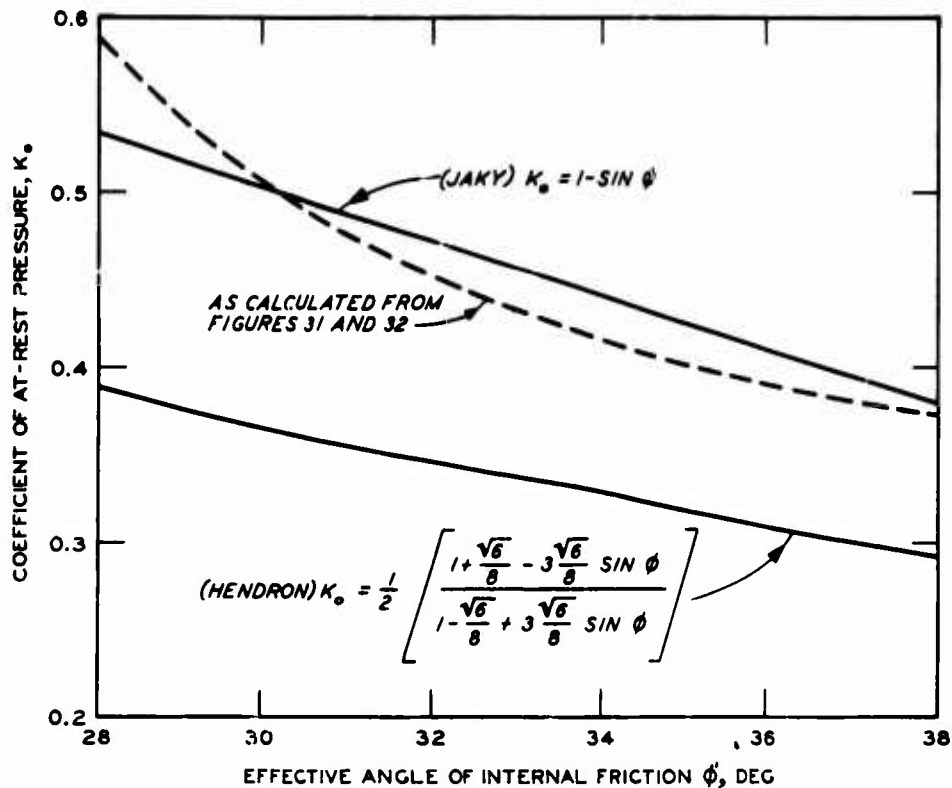


Figure 33. Relationship between the coefficient of earth pressure at rest K_o and the friction angle ϕ as obtained from consolidated-drained direct shear test for Reid-Bedford sand

relationship suggested by Jaky²⁹ but are higher than the one suggested by Hendron.⁶

Stress-Strain Relationship

52. The stress-strain measurements for the Reid-Bedford sand under uniaxial strain are presented in Figures 27-30. These curves show nonlinear characteristics for the entire range of densities tested. The steepness of each curve is dictated by its density; the denser the sand, the steeper the curve. The nonlinearity of the stress-strain curves for the sand tested is also influenced by the stress level; the higher the stress level, the steeper the curve. The curvature of the stress-strain curve is usually measured by the "constrained modulus" of deformation, D . The constrained tangent modulus of deformation which, by definition,

is the ratio of axial stress with respect to strain under zero lateral strain may be expressed as:

$$D = \frac{d \sigma_a}{d \epsilon_a} \quad (12)$$

where ϵ_a is the axial strain.

For linear elastic materials, D may be expressed in terms of the modulus of elasticity E and Poisson's ratio ν , as:

$$D = \frac{E(1 - \nu)}{(1 + \nu)(1 - 2\nu)} \quad (13)$$

or the value E can be expressed in terms of D and K_o as:

$$E = \frac{D(1 + 2K_o)(1 - K_o)}{(1 + K_o)} \quad (14)$$

53. From Figures 27-30 it appears that the constrained modulus for the Reid-Bedford sand tends to increase with increasing density and increasing stress level used in the testing program. A general comparison of the stress-strain curves shows that tests with the swinging arms yielded the highest constrained modulus while the LVDT clamps yielded the lowest value. The burette method and the K_o belt with strain gages were second and third, respectively. The experimental stress-strain curves obtained may be approximated by an exponential function of the form:

$$\sigma_a = m\epsilon_a^n \quad (15)$$

where m and n are constant or they can be expressed by a rectangular hyperbola of the form:

$$\sigma_a = \frac{\epsilon_a}{a - b\epsilon_a} \quad (16)$$

where a and b are positive numbers. The experimental fit of the data is beyond the scope of this study.

54. In a previous study Durbin³³ conducted dynamic uniaxial compression and wave propagation tests on 1.5-in.-diam specimens of Reid-Bedford sand. These tests were compared at a comparable density with static K_0 tests conducted in this study, and the results are summarized in Figure 34. It appears from the figure that the stiffness of the sand in the static test is lower than that obtained from wave propagation or dynamic uniaxial compression tests. However, the difference is small enough so that K_0 test data from static tests may be used in a dynamic problem with reasonable accuracy. A comprehensive discussion of the effects of loading rate on the stiffness and strength of sand is beyond the scope of this report. This topic is summarized in recent reports by Whitman³⁴ and Isenberg.³⁵

Factors Affecting K_0 and Constrained Modulus

55. It has been shown earlier that the values of K_0 and the constrained modulus D are affected by the relative density and stress level, but they are only slightly influenced by the method used in restraining the lateral movement during the test and the rate of loading. However there are many other factors which may influence K_0 and D ; these factors are discussed in the following paragraphs.

Effect of lateral yielding

56. As early as 1934, Terzaghi¹ pointed out the importance of no lateral yielding on the measurement of earth pressure behind a retaining wall. Since that time it has been considered that small lateral strains, particularly when the soil sample is enclosed in a steel ring, as in the case of a conventional consolidometer, have a negligible effect on the value of K_0 . Research work credited to Speer by Fulton and Hendron³⁶ indicated that the lateral strain had a significant effect on the value of K_0 . Speer's results on sand presented in Figure 35 show that a lateral strain of 0.5×10^{-6} percent may cause a 10 percent reduction in the value of K_0 . However Andrawes and El-Sohby¹⁵ in a recent study on

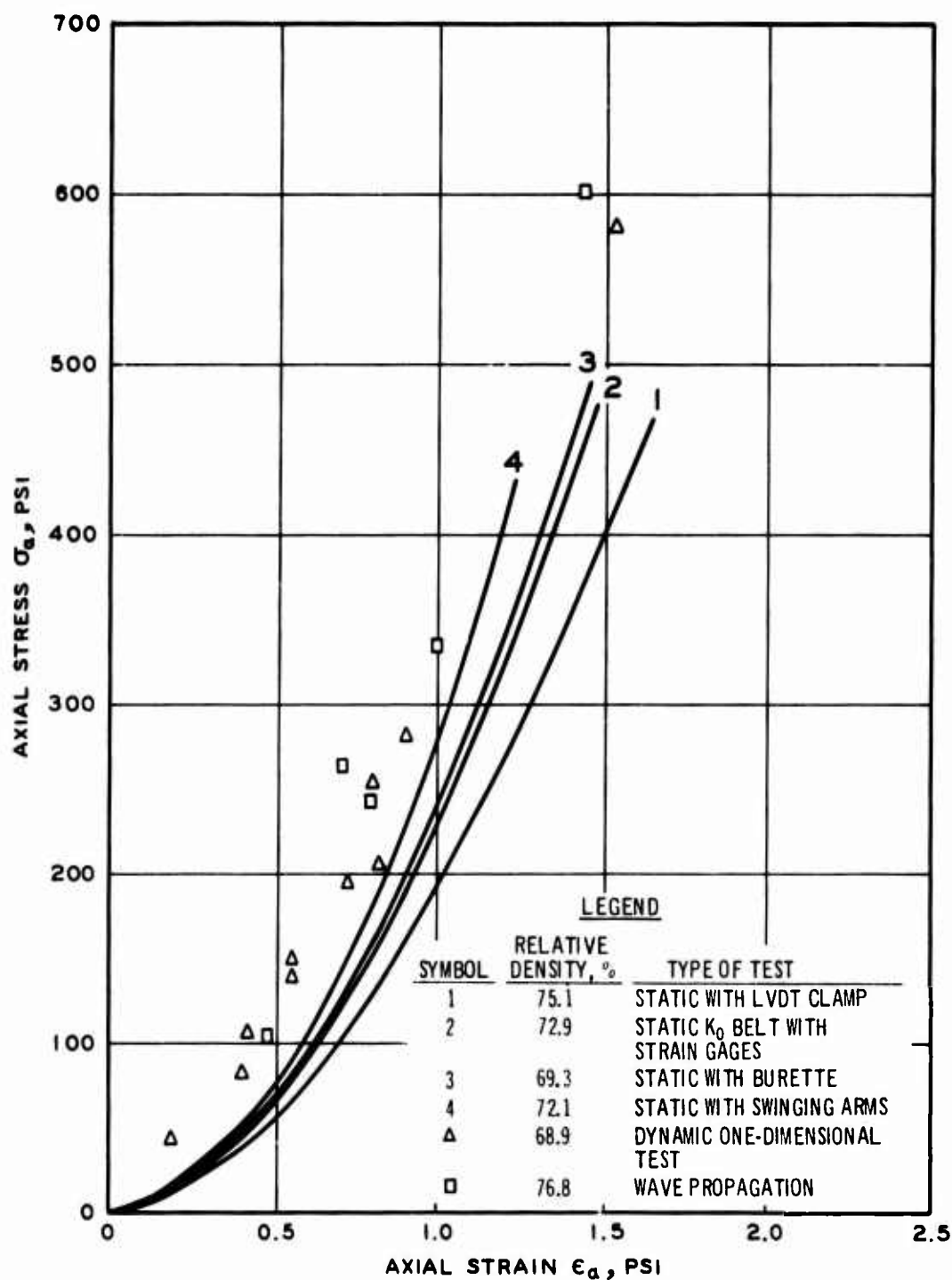


Figure 34. Comparison of static and dynamic stress-strain relationships for Reid-Bedford sand under K_0 condition

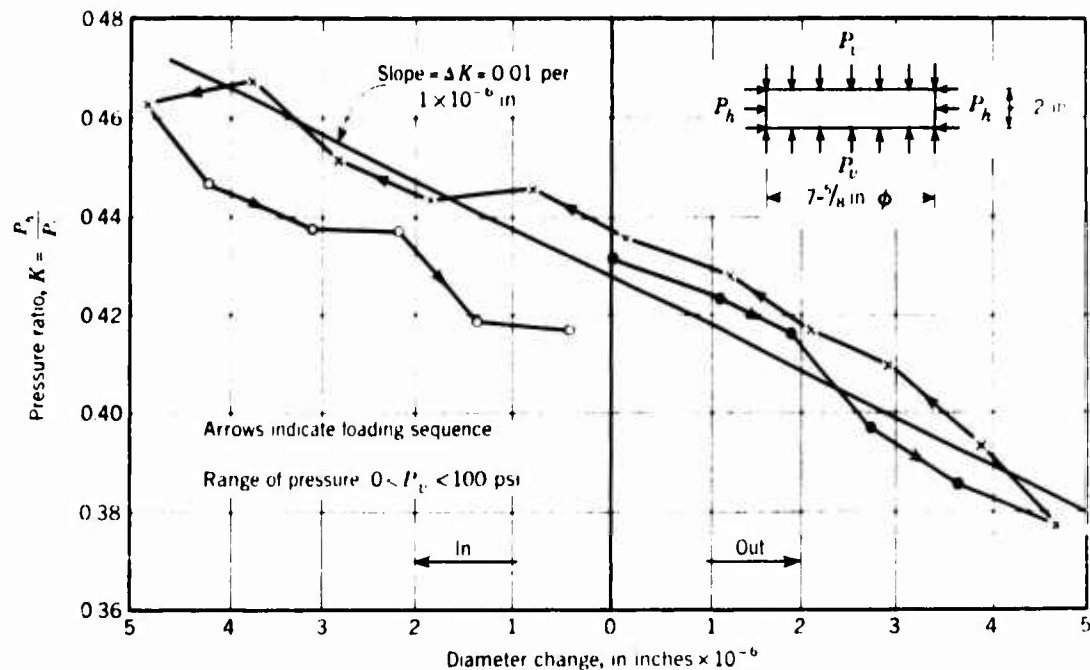


Figure 35. Effect of lateral motion on pressure ratio K for dry sand. Void ratio = 0.77 (after Speer³⁶)

dense glass ballotini of 0.1-mm diameter showed that K_0 is not significantly affected when the ratio between the axial stress and radial stress is within ± 0.1 of that required to maintain K_0 conditions. It might be possible that lateral yielding does not affect K_0 for a uniform material as in the case of glass ballotini while it influences K_0 for graded material as in the case of sand used in Speer's tests. More tests are needed to resolve this question. As far as is known there have been no published data that show the effect of lateral yielding on K_0 values in clay.

Effect of particle shape

57. In a previous study^{30,31} K_0 tests were conducted on two sands of identical grain-size distribution and relative density but with different particle shapes. The first sand was crushed basalt with highly angular particles, while the second sand, obtained from Painted Rock dam-site at Gila Bend, Arizona, had subrounded particles. The radial versus the axial stress data for these two sands under K_0 conditions are presented in Figure 36. It is apparent that angular sand has a higher

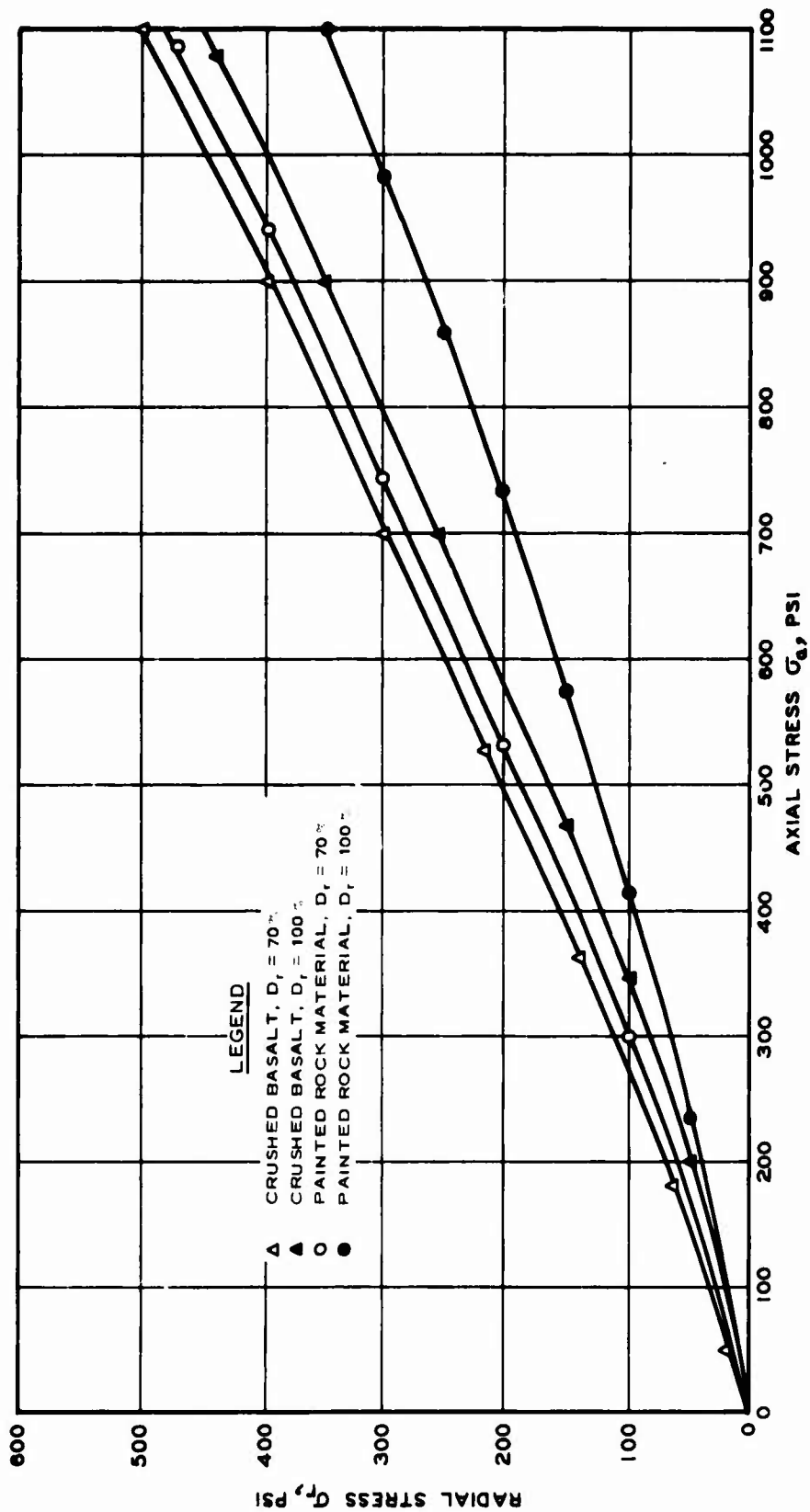


Figure 36. Radial versus axial stress during K_o consolidation for crushed basalt and Painted Rock Dam material

value of K_0 than rounded sand, and the difference decreases with decreasing density. Figure 37 shows the axial stress-strain relationship for these two sands and demonstrates that the constrained modulus for Painted Rock material is much higher than that of crushed basalt. This indicates that the constrained modulus decreases with increasing angularity of the particles.

Effect of unloading and reloading

58. The relationship between the radial and axial stresses for Reid-Bedford sand under repeated loading and unloading cycles using the LVDT clamps is shown in Figure 38. The relationship for the first loading cycle may be approximated by a straight line. However, upon unloading, the stress-strain relationship becomes nonlinear with a convex shape. The relationship during first reloading is also nonlinear and concave upward with a slope much flatter than the first loading cycle but steeper than the first unloading cycle. This trend was similar for the dense and loose specimens; however, the denser specimen exhibited a flatter slope than the loose specimen for any particular loading or unloading cycle. The results are presented in the following tabulation.

Stress Cycle	Variation of K_0 Value	
	$D_r = 100\%$	$D_r = 25\%$
1st loading	0.37	0.58
1st unloading	0.37 to 0.9	0.58 to 0.9
2nd loading	0.9 to 0.43	0.90 to 0.56
2nd unloading	0.43 to 1.0	0.56 to 0.90
3rd loading	0.43 to 1.0	0.90 to 0.55
3rd unloading	1.0 to 0.43	0.55 to 1.0

These results also indicate that K_0 is always lower on loading than unloading, and that K_0 varies with increasing number of loading cycles. The values of K_0 for different loading cycles when plotted as a function of the overconsolidation ratio (OCR) in Figure 39, show that K_0 increases progressively with increasing OCR in a manner which is independent of the loading cycle. From Figures 38 and 39 it is obvious that

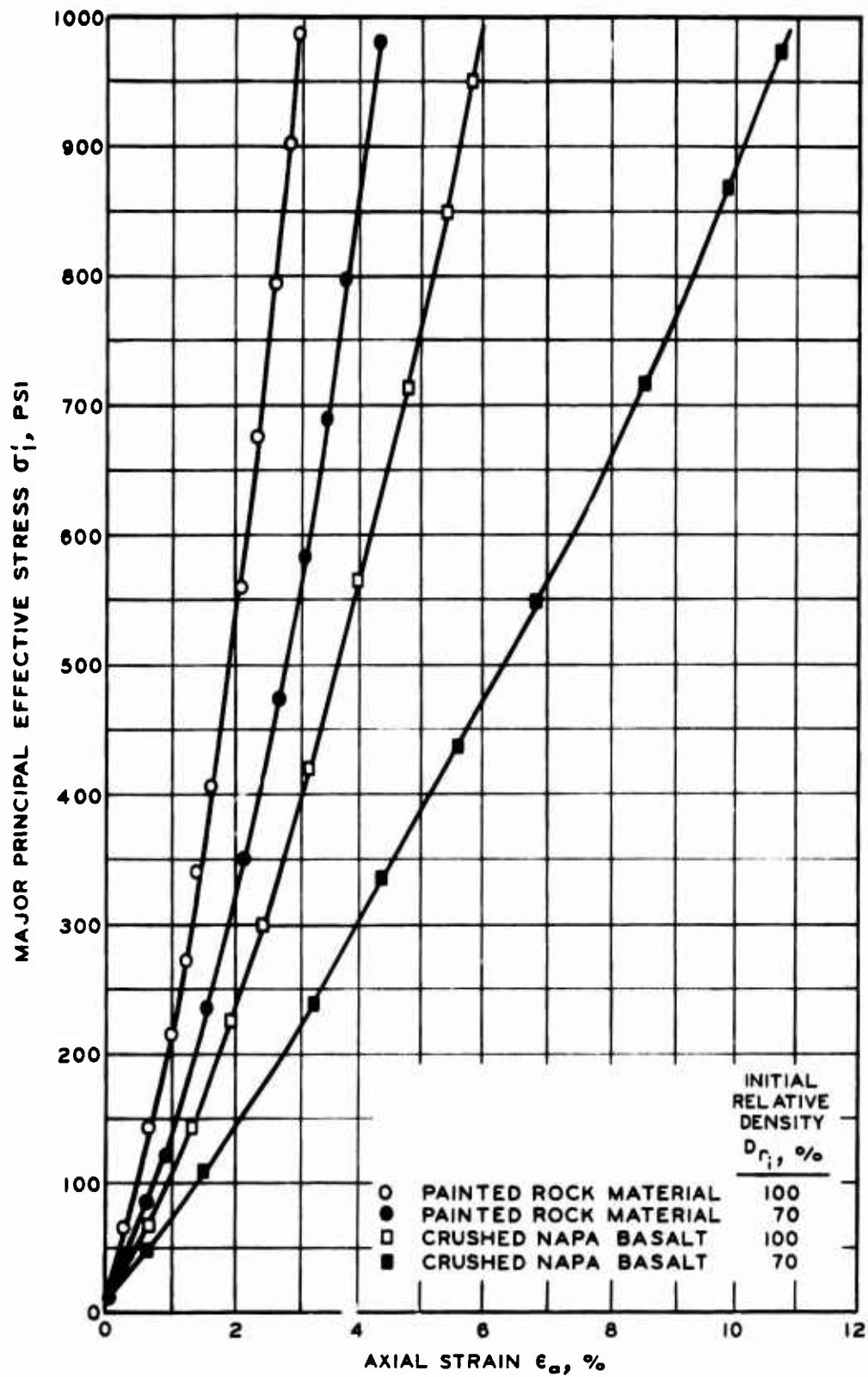


Figure 37. Stress-strain curve for triaxial specimens under K_0 consolidation (from Reference 32)

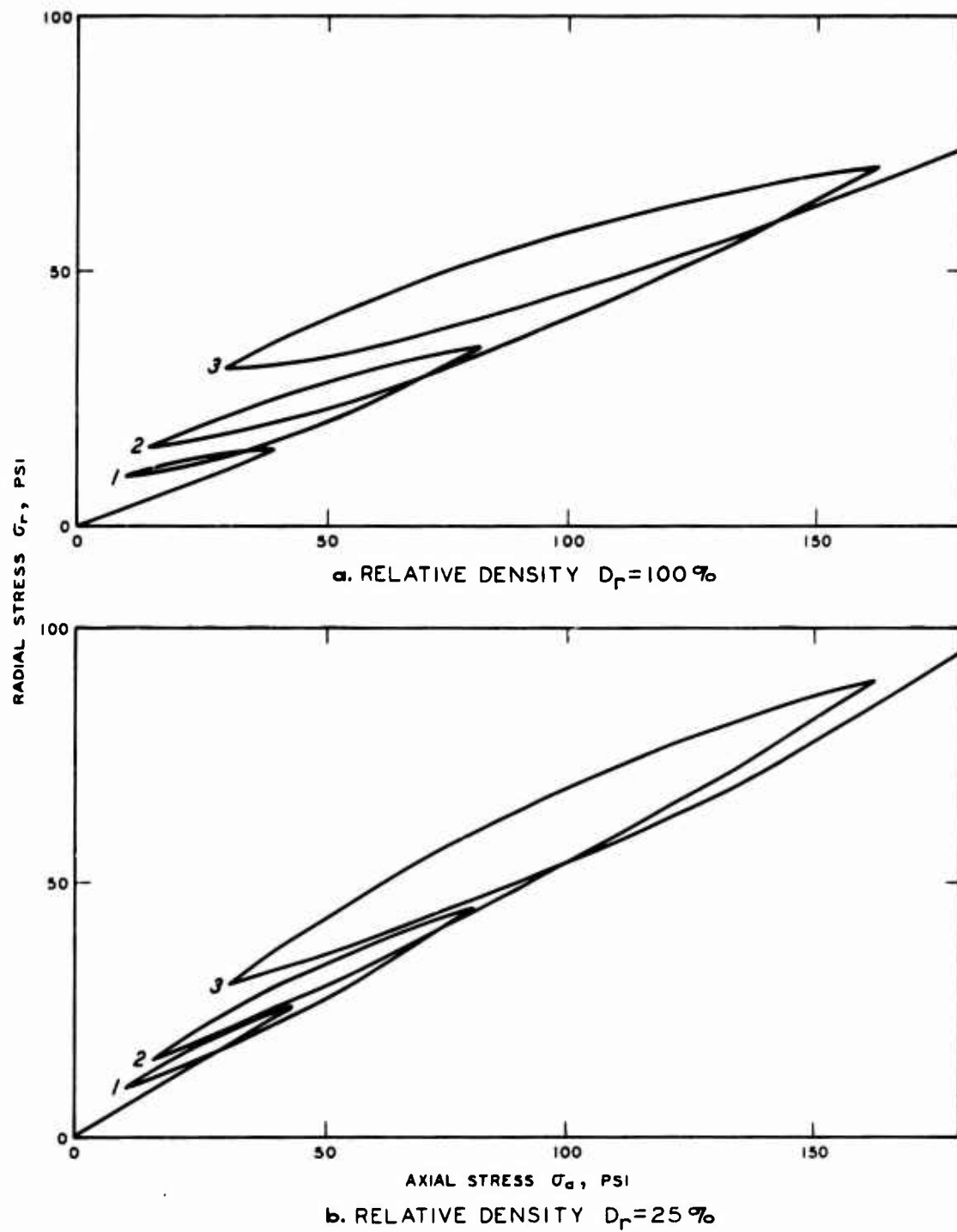
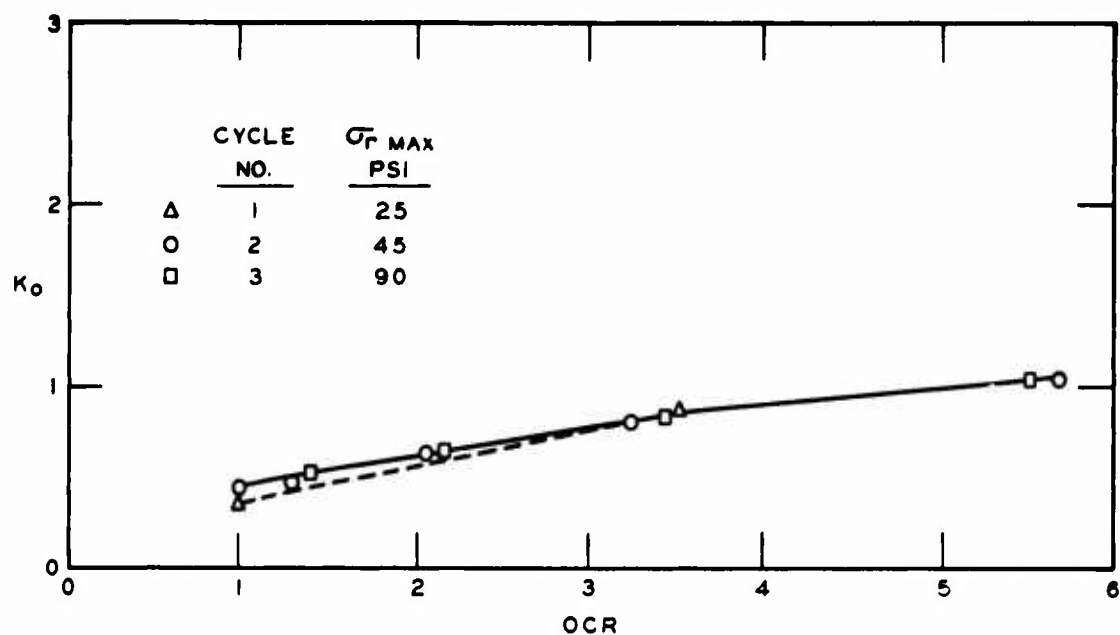
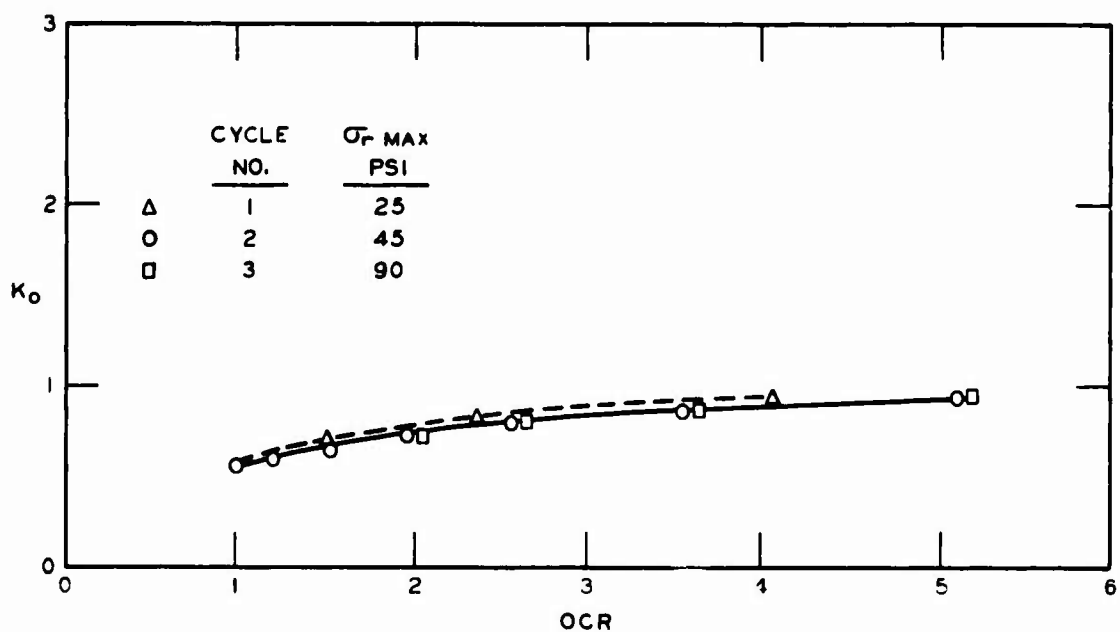


Figure 38. Radial versus axial stress for Reid-Bedford sand under K_0 condition during loading and unloading cycles using LVDT clamps



a. RELATIVE DENSITY $D_r = 100\%$



b. RELATIVE DENSITY $D_r = 25\%$

Figure 39. Relationship between K_o and the OCR

the value of K_o is influenced by stress history, a phenomenon which is more pronounced in cohesive soil.

59. The uniaxial stress-strain relationship for Reid-Bedford sand under loading and unloading cycles using the LVDT clamps is shown in Figure 40. The figure shows that the slope of the curve which defines the constrained modulus D is much higher on unloading than loading and that while D is increasing with increasing number of loading cycles, upon loading it has almost the same value for all unloading cycles. The constrained modulus for any loading or unloading cycles is much higher for dense than for loose specimens. Average values of D as affected by loading cycles are presented in the following tabulation.

Stress Cycle	Average Constrained	
	Modulus D , 10^4 psi	
	$D_r = 100\%$	$D_r = 25\%$
1st loading	2.75	0.75
1st unloading	4.60	3.90
2nd loading	3.25	1.45
2nd unloading	4.55	3.90
3rd loading	3.90	1.85
3rd unloading	4.55	4.80

Effect of stress level

60. At low stress levels the relationship between σ_r and σ_a under K_o consolidation is almost linear as indicated previously; however, at elevated pressures in tests using the LVDT clamp the relationship became nonlinear with a gradual increase and then decrease in the curvature as shown in Figure 41. This implies that there is a continuous increase in the value of K_o with increasing pressure and that such increase is more pronounced in dense sand than in loose sand. The following tabulation shows the effect of confining pressure, σ_r , on

Confining Pressure, σ_r , psi	K_o Loading	
	$D_r = 25\%$	$D_r = 100\%$
0 to 250	0.55	0.42
250 to 500	0.62	0.47
500 to 750	0.61	0.55
750 to 1000	0.61	0.54

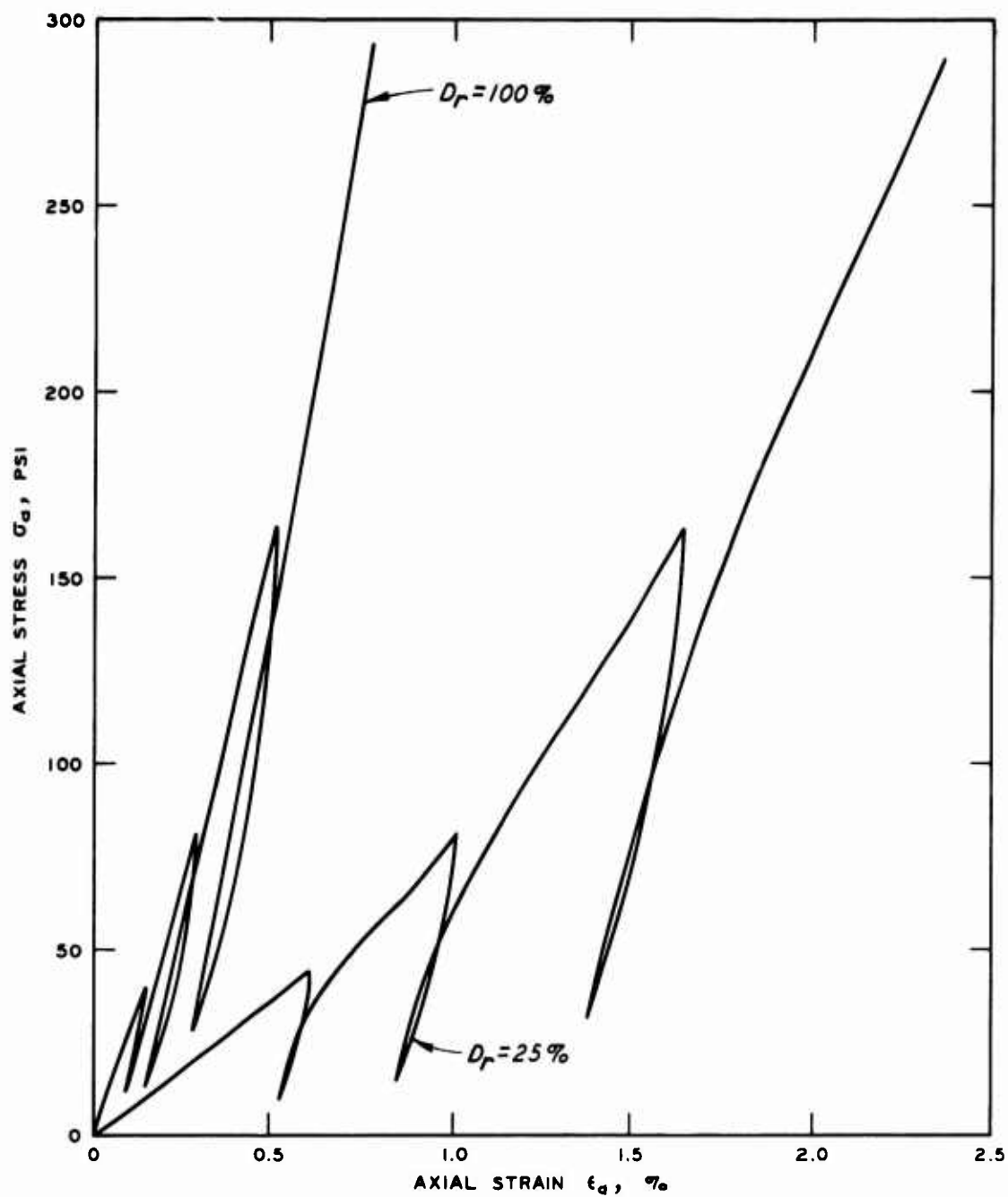


Figure 40. Axial stress-strain relationship for Reid-Bedford sand during loading and unloading cycles using LVDT clamps

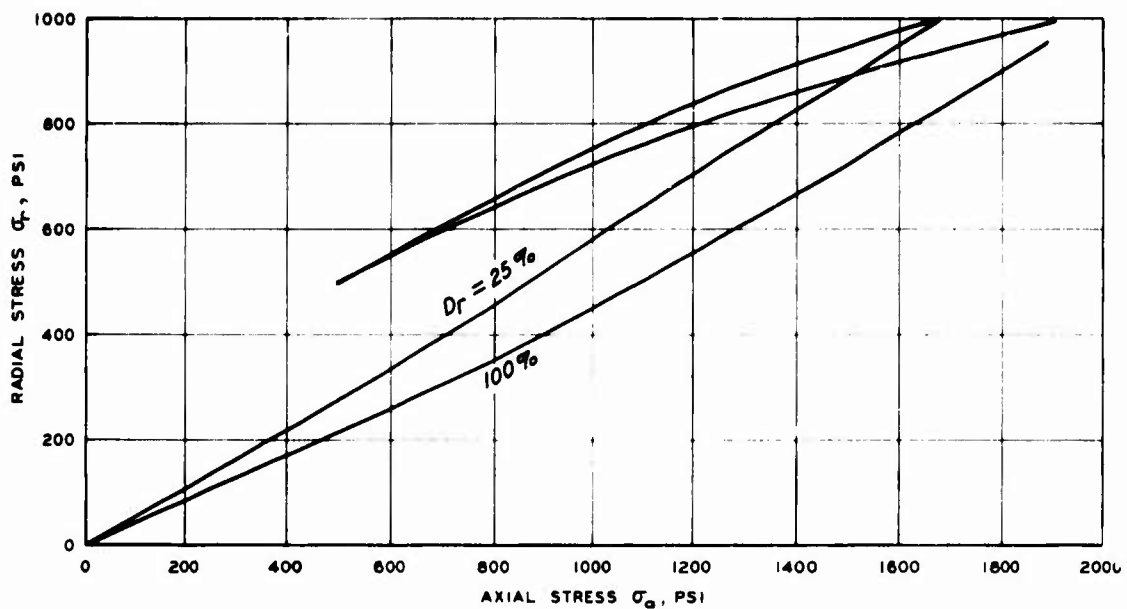


Figure 41. One-dimensional radial and axial relationship for Reid-Bedford sand and elevated pressure

the K_0 value. It may be possible that at very high pressures, with no significant grain crushing, both loose and dense sands assume the same value of K_0 . A plot of the stress path of a K_0 test as loading progresses is shown in Figure 42. The figure shows that the stress paths for both dense and loose sand are nonlinear and concave downward with dense sand having more curvature than loose sand.

61. High pressures not only affect the value of K_0 but also influence the magnitude of the constrained modulus, D . Figure 43 shows the axial stress-strain relationship for dense and loose specimens consolidated under K_0 condition to a confining pressure of 1000 psi. It might be noted that while D is higher for dense than for loose sand upon loading, for the range of confining pressures used in these tests, however, the value of D is about the same for both densities upon unloading.

62. The figure also shows that the curvature of both curves appears to change continuously; while these curves are linear or concave upward to low stress level, they are concave downward at high stress level. This means that the constrained modulus D increases with

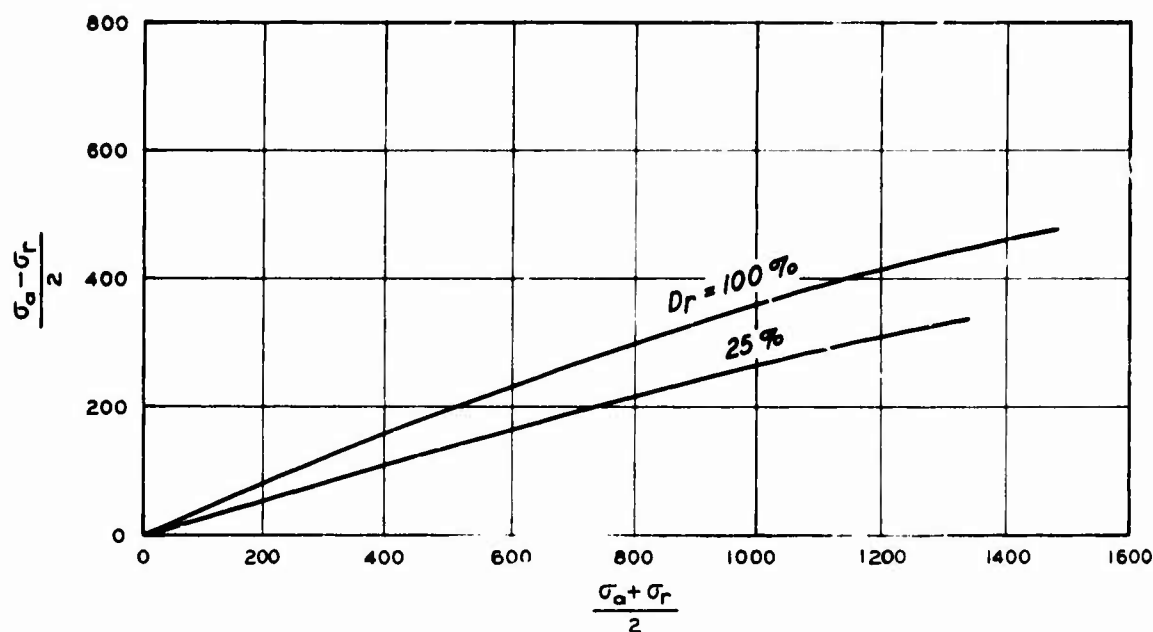


Figure 42. Stress path for Reid-Bedford sand under K_0 conditions

increasing stress level until it reaches a maximum value then it starts to decrease continuously with increasing confining pressure. This decrease in D may in part be due to crushing of the sand grains. A previous study by Chisolm³⁷ on Reid-Bedford sand tested under axial stresses up to 10,000 psi has shown that significant grain crushing occurs at axial stresses in excess of 2,000 psi. He observed that when crushing of grains began, the uniaxial stress-strain curve underwent a softening effect as shown in Figure 44. This softening varied with the density of the sand tested. Unfortunately, it is not possible to separate the effect of stress level from grain crushing on the value of K_0 with present-day techniques.

Effect of mineralogy and fines

63. It is known that the stress-strain characteristics of granular soil are affected by the elastic properties of the mineral from which it is composed. Thus, it is likely that the value of K_0 is affected by the elastic property of the mineral particles. Unfortunately, there are no published data to support this supposition; however, tests on similar specimens with different mineral composition may resolve this

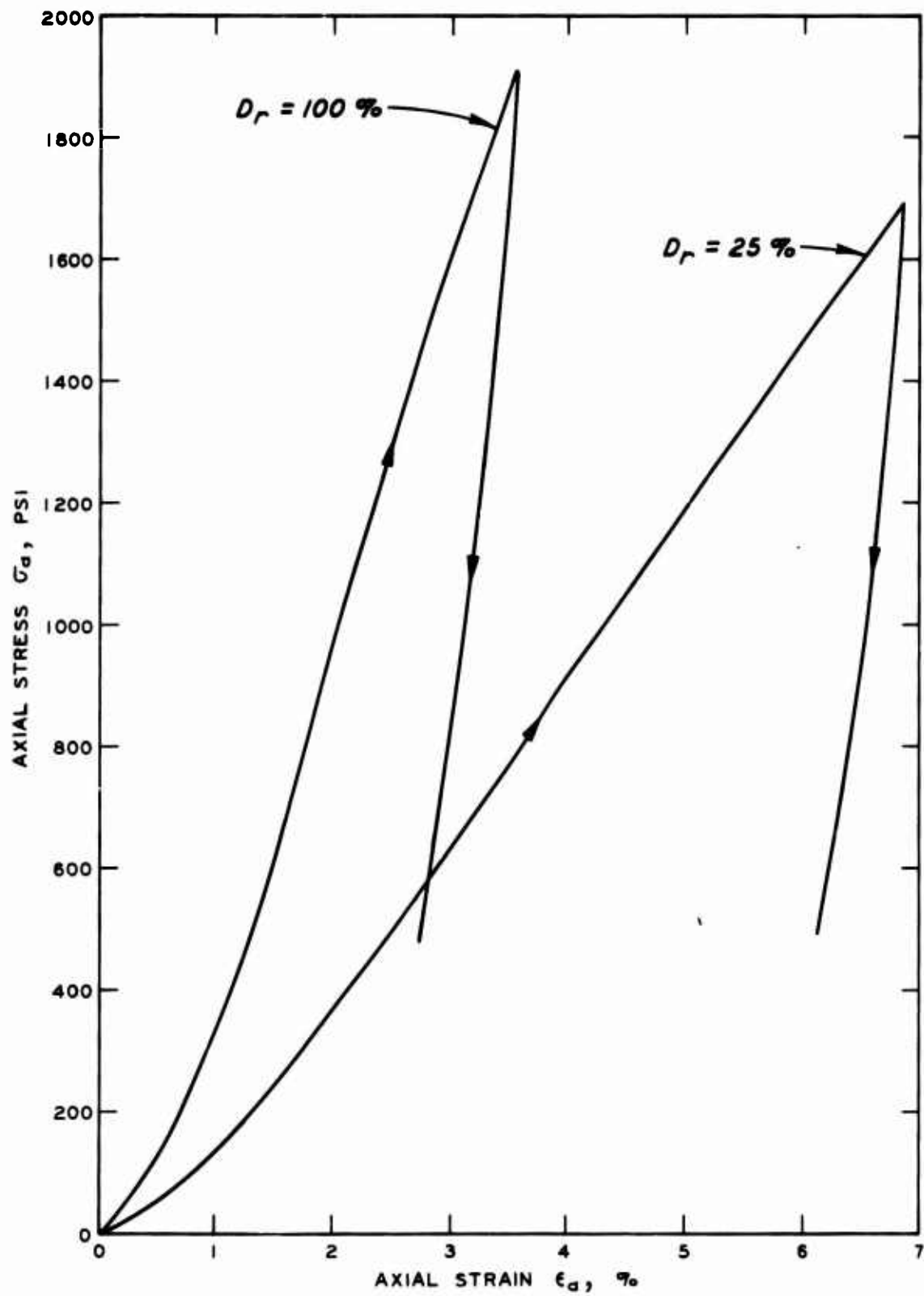


Figure 43. Uniaxial stress-strain relationship for Reid-Bedford sand under high pressure using LVDT clamps

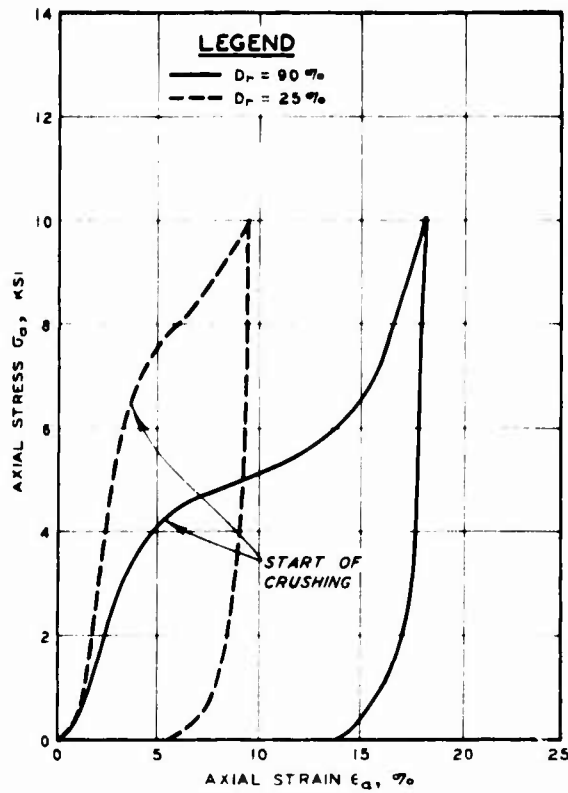


Figure 44. Effect of grain crushing on the stress-strain relationship of Reid-Bedford sand

question. The presence of fines in granular material also influences the value of K_0 ; however, the amount of variation in K_0 due to the presence of fines is not well established. Previous tests by Moore¹³ show that the value of K_0 in silt increases with increase in mica content.

PART V: CONCLUSIONS AND RECOMMENDATIONS

Conclusions

64. Within the bounds of this investigation (the testing methods employed, the material tested, and the procedures and equipment used), the following conclusions are drawn:

- a. The value of K_0 for Reid-Bedford sand was found to be practically the same irrespective of the method used in maintaining no radial deformations of the specimen. The LVDT clamp, K_0 belt, swinging arm lateral strain sensors, and the indirect burette method all produced comparable K_0 values for relative densities ranging from 25 to 99 percent. The K_0 belt tended to give the highest K_0 values while the swinging arms lateral strain sensor indicated the lowest values. The LVDT clamp is preferred for laboratory testing since it is easier to use and maintain and also provides reliable results.
- b. The experimentally derived K_0 values agree well with Jaky's²⁹ theoretical equation:

$$K_0 = 1 - \sin \phi$$

while Hendron's⁶ equation underestimated the experimental values.

- c. K_0 values determined by dynamic and wave propagation techniques conducted previously by Durbin³³ agree well with those determined statically in this study. Hence K_0 and the stress-strain relationships of Reid-Bedford sand under K_0 conditions are only slightly affected by the rate of loading, and statically determined K_0 values and stress-strain relationships may be used for dynamic problems.
- d. K_0 values are lower on loading than on unloading and vary with increasing number of loading cycles. Thus K_0 is influenced by the stress history.
- e. K_0 increases with increasing stress level for dense sand and remains almost unchanged for loose sand.
- f. The constrained modulus, D , of Reid-Bedford sand increases with increasing density and increasing stress level. The swinging arms lateral strain sensor gave the highest constrained modulus values while the

LVDT clamp lateral strain sensor gave the lowest.

- g. The constrained modulus, D , increases with increasing numbers of loading cycles, is much higher on unloading, and has almost the same value for each unloading cycle.

Recommendations

65. With regard to further development of the findings of this study, it is recommended that:

- a. A study be made of the effect of rate of strain, grain crushing, and the presence of fines on the value of K_o in granular soil.
- b. A similar study be conducted on cohesive soils.

REFERENCES

1. Terzaghi, K., "Large Retaining Wall Test," Engineering News Record, Vol 112, 1934, pp 136-140.
2. Rinkert, A., "Measurement of the Pressure of Filling Materials Against Walls," Proceedings, Royal Swedish Geotechnical Institute, No. 17, 1959.
3. Mackey, R. D. and Kirk, D. P., "At Rest, Active and Passive Earth Pressures," Proceedings, Southeast Asian Regional Conference on Soil Engineering, Apr 1967, pp 187-198.
4. Terzaghi, K., "Old Earth Pressure Theories and New Test Results," Engineering News Record, Vol 85, No. 14, 1920, pp 632-637.
5. Kjellman, W., "Report on an Apparatus for the Consumate Investigation of the Mechanical Properties of Soils," Proceedings, First International Conference on Soil Mechanics and Foundation Engineering, Vol II, 1936, pp 16-20.
6. Hendron, A. J., The Behavior of Sand in One-Dimensional Compression, Ph. D. Thesis, 1963, University of Illinois, Urbana, Ill.
7. Brooker, E. W. and Ireland, H. O., "Earth Pressure at Rest Related to Stress History," Canadian Geotechnical Journal, Vol 11, No. 1, 1965, p 1.
8. Murdock, L. J., "Consolidation Tests on Soils Containing Stones," Proceedings, Second International Conference on Soil Mechanics and Foundation Engineering, Vol 1, 1948, pp 169-173.
9. Bishop, A. W., "Discussion," Proceedings, Brussels Conference on Earth Pressure Problems, Vol III, Sep 1958, pp 36-39.
10. Terrel, R. L., Factors Influencing the Resilient Characteristics of Asphalt Treated Aggregates, Ph. D. Thesis, 1967, University of California, Berkeley, Calif.
11. Dehlen, G. L., The Effect of Nonlinear Material Response on the Behavior of Pavement Subjected to Traffic Load, Ph. D. Thesis, 1969, University of California, Berkeley, Calif.
12. Al-Hussaini, M. M., "The Influence of End Restraint and Method of Consolidation on the Drained Triaxial Compressive Strength of Crushed Napa Basalt," Miscellaneous Paper S-70-18, June 1970, U. S. Army Engineer Waterways Experiment Station, CE, Vicksburg, Miss.
13. Moore, C. A., "Effect of Mica on K_0 Compressibility of Two Soils," Journal, Soil Mechanics and Foundation Division, American Society of Civil Engineers, Vol 97, No. SM9, 1971, pp 1275-1289.
14. Bishop, A. W. and Eldin, A. K., "The Effect of Stress History on the Relation Between K_0 and Porosity in Sand," Proceedings, Third International Conference on Soil Mechanics and Foundation Engineering, Vol I, 1953, pp 100-105.

15. Andrawes, K. Z. and El-Sohby, M. A., "Factors Affecting Coefficient of Earth Pressure K_0 ," Journal, Soil Mechanics and Foundation Division, American Society of Civil Engineers, Vol 99, SM7, 1973, pp 527-538.
16. Holtz, R. D., "Discussion: Use of Servo Mechanism for Volume Change Measurement and K_0 Consolidation," Geotechnique, Vol XXII, No. 2, Jun 1972, pp 371-372.
17. Bishop, A. W., Webb, D. L., and Skinner, A. E., "Triaxial Test on Soil at Elevated Cell Pressure," Proceedings, Sixth International Conference on Soil Mechanics and Foundation Engineering, Vol 1, 1965, pp 170-174.
18. Kjellman, W. and Jakobson, B., "Some Relations Between Stress and Strains in Coarse-Grained Cohesionless Materials," Proceedings, Royal Swedish Geotechnical Institute, No. 9, 1955.
19. Gilbert, P. A. and Townsend, F. C., "Use of Bison Strain Gages in Triaxial Testing" (unpublished data), Feb 1972, U. S. Army Engineer Waterways Experiment Station, CE, Vicksburg, Miss.
20. Bison Instruments, Inc., "Soil Strain Gage Model 4101A," Instruction Manual.
21. Mazanti, B. B. and Holland, C. N., "Study of Soil Behavior Under High Pressure; Response of Two Recomacted Soils to Various Stages of Stress," Contract Report S-70-2, Report 1, Vol 1, Feb 1970, U. S. Army Engineer Waterways Experiment Station, CE, Vicksburg, Miss., prepared by Georgia Institute of Technology under Contract No. DACA 39-67-C-0051.
22. Ehrgott, J. Q., "Calculation of Stress and Strain from Triaxial Test Data on Undrained Soil Specimen," Miscellaneous Paper S-71-9, May 1971, U. S. Army Engineer Waterways Experiment Station, CE, Vicksburg, Miss.
23. Wroth, C. P. and Hughes, J. M. O., "An Instrument for the In-Situ Measurement of the Properties of Soft Clays," Proceedings, Eighth International Conference on Soil Mechanics and Foundation Engineering, Vol 1.2, 1973, pp 487-494.
24. Bjerrum, L. and Anderson, K. H., "In Situ Measurement of Lateral Pressure in Clay," Proceedings, Fifth European Conference on Soil Mechanics and Foundation Engineering, Vol 1, 1972, pp 11-20.
25. Penman, A. D. M., "Discussion," Proceedings, Fifth European Conference on Soil Mechanics and Foundation Engineering, Vol 2, 1972, p 87.
26. Vaughan, P. R., "Discussion," Proceedings, Fifth European Conference on Soil Mechanics and Foundation Engineering, Vol 2, 1972, pp 72-75.
27. Fry, Z. B., "A Procedure for Determining Elastic Moduli of Soils by Field Vibratory Technique," Miscellaneous Paper No. 4-577, Jun 1963, U. S. Army Engineer Waterways Experiment Station, CE, Vicksburg, Miss.

28. Richart, F. E., Jr., "Foundation Vibrations," Journal, Soil Mechanics and Foundations Division, American Society of Civil Engineers, Vol 86, Part 1, No. SM4, Aug 1960, pp 1-34.
29. Jaky, J., "The Coefficient of Earth Pressure at Rest," Journal, Society of Hungarian Architects and Engineers, Budapest, Hungary, 1944, pp 355-358.
30. Al-Hussaini, M., "Investigation of Plane Strain Shear Testing; Plane Strain and Triaxial Compression Tests on Painted Rock Dam Material," Technical Report S-71-2, Report 3, Sep 1972, U. S. Army Engineer Waterways Experiment Station, CE, Vicksburg, Miss.
31. _____, "Investigation of Plane Strain Shear Testing; Drained Plane Strain and Triaxial Compression Tests on Crushed Napa Basalt," Technical Report S-71-2, Report 2, Jun 1971, U. S. Army Engineer Waterways Experiment Station, CE, Vicksburg, Miss.
32. Kennedy, T. E., Albritton, G. E., and Walker, R. E., "Initial Evaluation of the Free-Field Response of the Large Blast Load Generator," Technical Report No. 1-723, Jun 1966, U. S. Army Engineer Waterways Experiment Station, CE, Vicksburg, Miss.
33. Durbin, W. L., "Study of the Dynamic Stress-Strain and Wave-Propagation Characteristics of Soils; Measurements of Stress-Strain, Peak Particle Velocity, and Wave-Propagation Velocity in Three Sands," Contract Report No. 3-91, Report 3, Feb 1965, U. S. Army Engineer Waterways Experiment Station, CE, Vicksburg, Miss., prepared by United Research Services, Inc., under Contract No. DA-22-079-eng-373.
34. Whitman, R. V., "The Response of Soils to Dynamic Loadings; Final Report," Contract Report No. 3-26, Report 26, May 1970, U. S. Army Engineer Waterways Experiment Station, CE, Vicksburg, Miss., prepared by Massachusetts Institute of Technology under Contract No. DA-22-079-eng-224.
35. Isenberg, J., "Nuclear Geoplosics, A Sourcebook of Underground Phenomena and Effects of Nuclear Weapons, Part 2, Mechanical Properties of Earth Materials," DNA 1285H2, Nov 1972, Defense Nuclear Agency, Washington, D. C.
36. Fulton, R. E. and Hendron, A. J., "Discussion of Impact Waves in Sand: Theory Compared with Experiments on Sand Columns," Journal, Soil Mechanics and Foundations Division, American Society of Civil Engineers, Vol 87, No. SM6, 1961, pp 69-73.
37. Chisolm, E. E., "Behavior of Granular Materials Under High Stresses" (unpublished data), Apr 1971, U. S. Army Engineer Waterways Experiment Station, CE, Vicksburg, Miss.

APPENDIX A: NOTATION

a,b	Positive numbers
D	Constrained modulus of deformation
D_r	Relative density
E	Elastic modulus
f	Coefficient of friction at point of contact between spheres
g	Gravity acceleration
G	Shear modulus
h	Depth of the fill
K_o	Coefficient of earth pressure at rest
m,n	Constants
V_c	Compression wave velocity
V_s	Shear wave velocity
γ	In situ unit weight of soil
ϵ_a	Axial strain
ν	Poisson's ratio
σ_a	Average axial stress
σ_r	Radial stress
σ_1	Major principal stress
σ_3	Minor principal stress
ϕ	Failure angle
ϕ'	Effective angle of internal friction